# Particle and Plasma Diagnostics

Joel Fajans

Winter School on Physics with Trapped Charged Particles
19-30 January 2015

Ecole de Physique des Houches
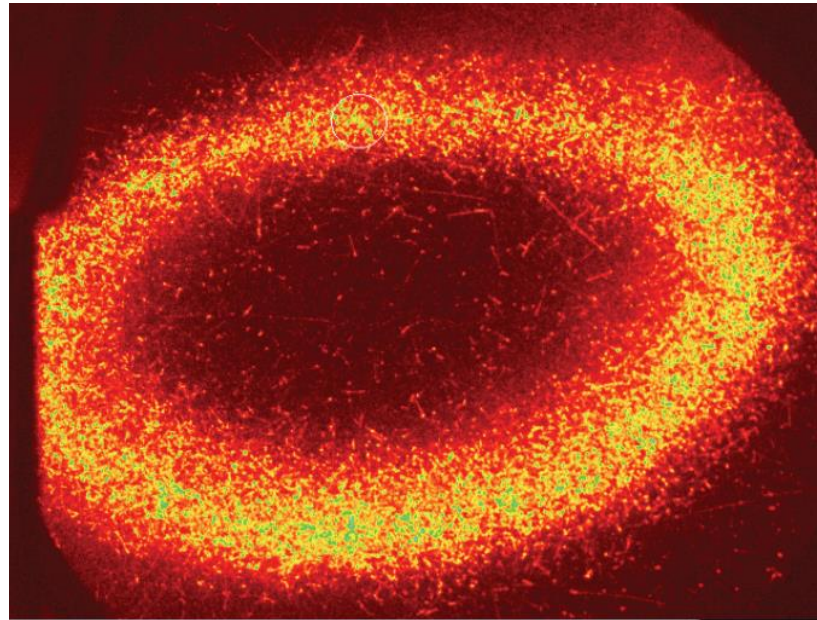
Hollow antiproton plasma imaged on a microchannel plate,
ALPHA 2012

How Do You Make a Particle/Plasma Experiment Work?
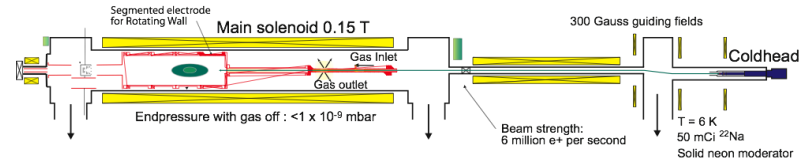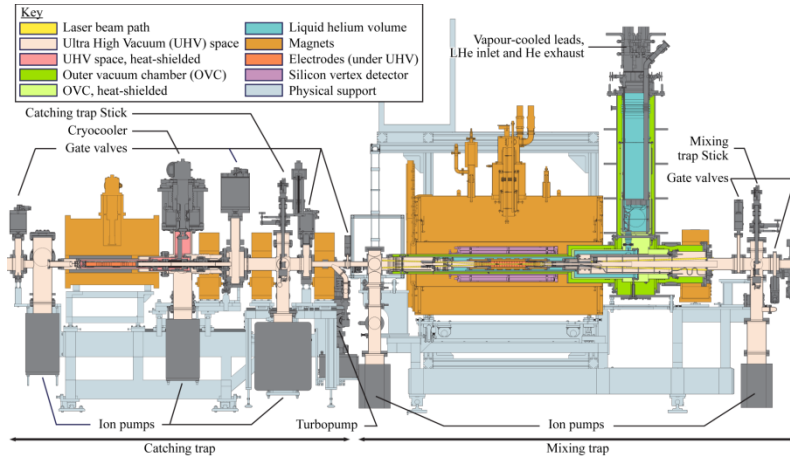

Surko-Style Positron Accumulator

ALPHA-II Antihydrogen Apparatus
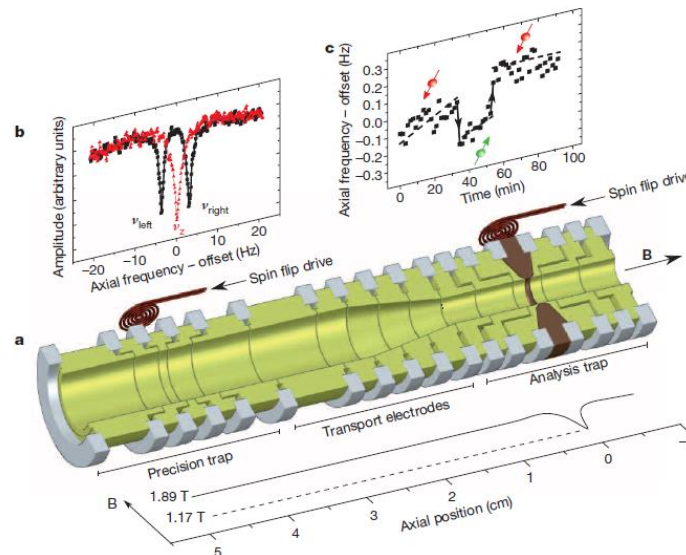
BASE (Anti)Proton Magnetic Moment Apparatus

Interesting Parameters

- Things we would like to know:
    - Particle Number.
        - Typical range: 10^3 to 10^9.
    - What type of particles are present?
        - Electrons, positrons, antiprotons, ions…
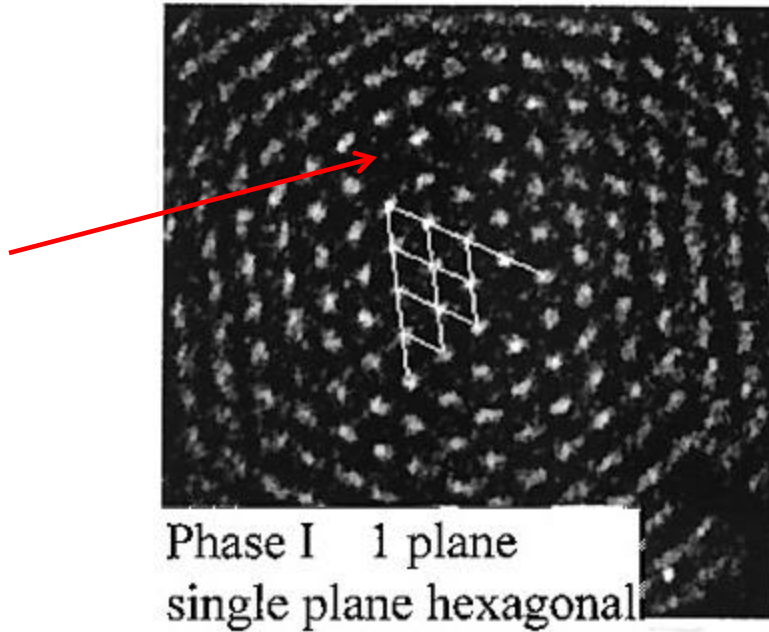
T. B. Mitchell, J. J. Bollinger, D. H. E. Dubin, X.-P. Huang, W. M. Itano,
R. H. Baughman, *Science*,**282** 1290 (1998)

Interesting Parameters

- Things we would like to know:
    - Particle Number.
        - Typical range: 10^3 to 10^9.
    - What type of particles are present?
        - Electrons, positrons, antiprotons, ions…
    - Radial Profile.
        - Typical range: 0.2mm to 10cm.
   - Can the system be parameterized by a single number, i.e. the radius?
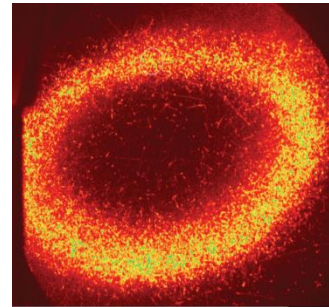
Interesting Parameters

- Things we would like to know:
  - Particle Number.
    - Typical range: 10^3 to 10^9.
  - What type of particles are present?
    - Electrons, positrons, antiprotons, ions...
  - Radial Profile.
    - Typical range: 0.2mm to 10cm.
    - Can system be parameterized by a single number, i.e. the radius?
  - Length.
    - Typical range: 0.5cm to 100cm.
  - Density
    - Typical range: 10^3 to 10^9cm^{-3}.
  - Temperature
    - Typical range 10 to 10^7K (0.5meV to 1000eV).
    - Can system be parameterized by a single number, i.e. the temperature?
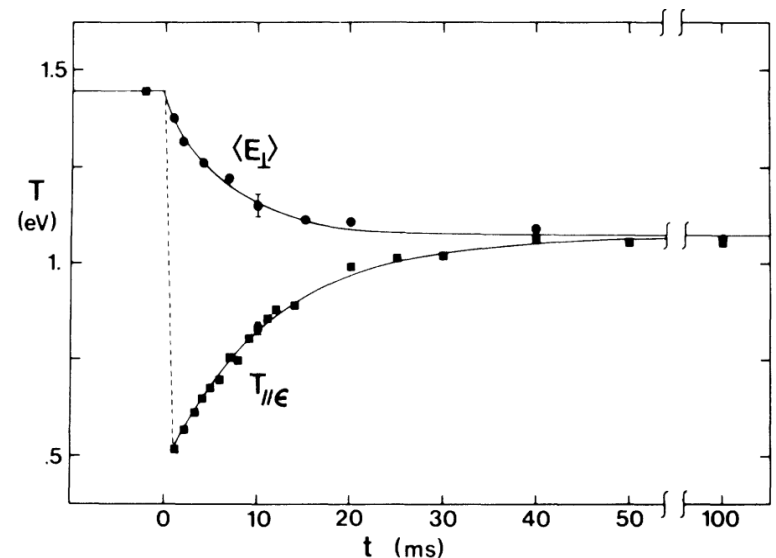
A.W. Hyatt, C.F. Driscoll and J.H. Malmberg "Measurement of the Anisotropic Temperature Relaxation Rate in a Pure Electron Plasma," Phys. Rev. Lett. **59**, 2975 (1987)

# Destructive vs. Nondestructive Diagnostics

- Nondestructive:
  - Advantages
    - Can work with the plasmas afterwards.
  - Disadvantages
    - Can be slow.
    - Can leave a wave imposed on the plasmas.
    - Can heat the plasmas.
    - May be difficult to calibrate.
- Destructive:
  - Advantages
    - Sometimes easier to calibrate.
  - Disadvantages
    - Destroys the plasmas.
    - Because the plasmas are changed radically, may have large systematic errors.

Non-Laser Based Diagnostics

- Concentrate on particles/plasmas for which laser diagnostics don't work.
  - Electrons, positrons, protons, antiprotons.

Particle Counting-Faraday Cups

- Faraday cups are used to count charged particles.
    - Have been in use for a very long time.
    - Basic design is very simple.

Secondary electron suppressor   Charge collection cup

Ion beam entrance   Electrical connection

Grounded shield

http://www.spectroscopyonline.com/detecting-ions-mass-spectrometers-faraday-cup
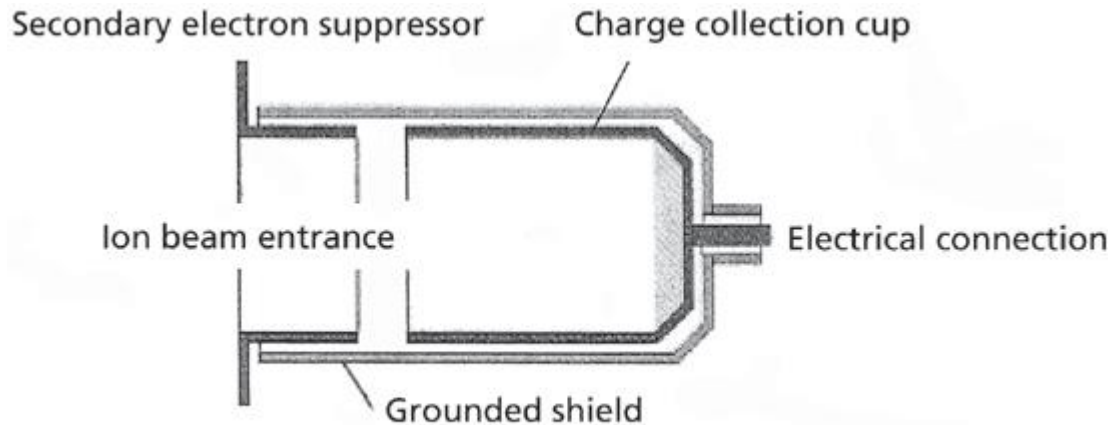
- Principal parts:
    - Charge collection cup: Self evident.
    - Grounded shield: Self evident
    - Secondary electron suppressor:
        - When the primary charged particle hit the cup, secondary electrons may be emitted
        - Secondary electron suppressor is biased negative relative to the charge collection cup.
        - Sends secondary electrons back to the cup.

Why are Faraday Cups Called Faraday Cups?

C

A

B

E
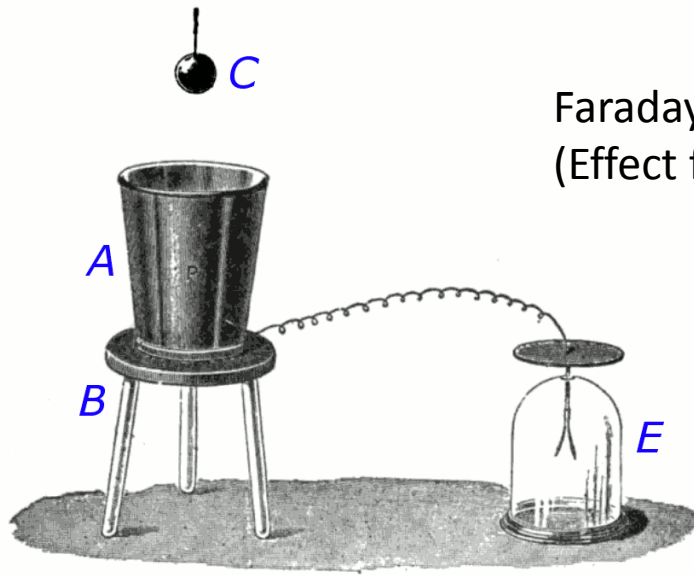
Faraday's Ice Pail
(Effect first observed by Benjamin Franklin in 1755)

http://en.wikipedia.org/wiki/Faraday's_ice_pail_experiment
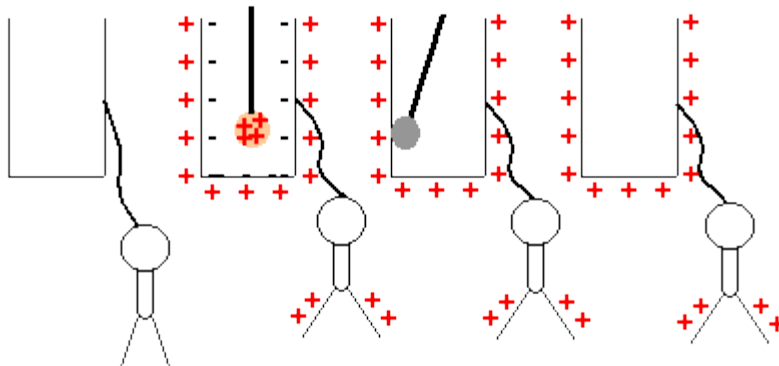
http://dev.physicslab.org/Document.aspx?doctype=3&filename=Electrostatics_ShellsConductors.xml

Faraday Cup Implementation

Complicated

Simple

Faraday Cup Circuit

Circuit Model
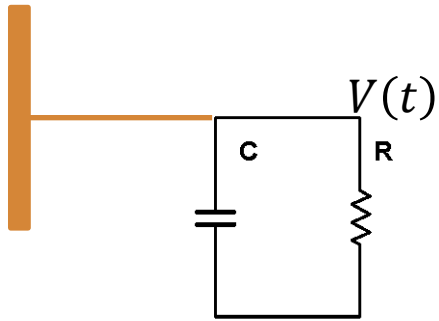
$$V_{\max} = \frac{Q}{C}$$

Q is the charge deposited on the plate.

$$\tau = RC$$

$$V(t) = V_{\max}\exp(-t/\tau)$$

Typical Circuit Response (ALPHA)

Faraday Cup Noise

Circuit Model

$V(t)$

C   R
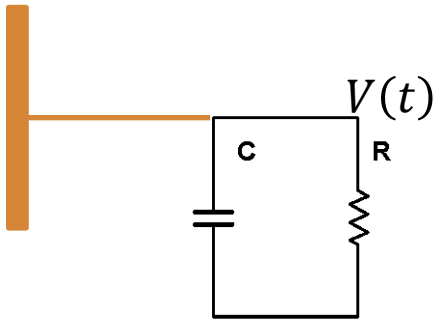
- Noise sources:
  - Thermal (Johnson or Nyquist) noise.
    - Johnson Noise
      $V_N = \sqrt{4k_B T R B}$, where B is the bandwidth in which the signal is measured
   - Total noise on plate is independent of the resistor
      $V_N = \sqrt{\dfrac{k_B T}{C}}$.
    - Capacitance comes from cable and cup.
    - Typical capacitance is 1nF.
      - This yields $2\mu V$ of noise, or 12500e.

Faraday Cup Noise

Circuit Model
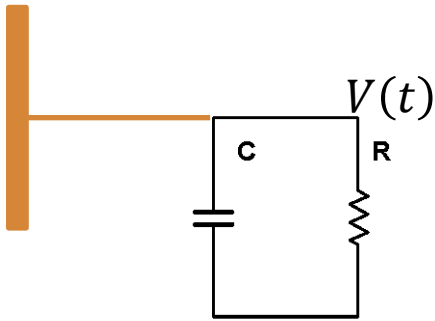


- Noise sources:
    - Thermal (Johnson or Nyquist) noise.
        - This yields 2μV of noise, or 12500e.
    - Amplifier Noise
        - Typical amplifier bandwidth might be 100kHz.
        - Typical amplifier noise might be $2\text{nV}/\sqrt{\text{Hz}}$
            - This yields a 0.6μV of noise, or 3750e.

For these parameters, thermal noise dominates.

# Faraday Cup Noise

Circuit Model

$V(t)$

C   R
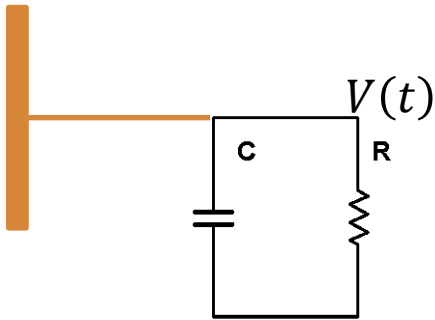
- Actual Noise: about 200k electrons.
- Where does the noise come from?
  - 50/60Hz coupling.
  - Noise pickup from nearby cables.
  - Accidental "thermocouple" junctions.
  - Bad solder joints.
  - Bad connectors.
  - Triboelectric effect.
    - System acts like a microphone.

Typical Circuit Response (ALPHA)

Triboelectric Noise Test

5' of test cable between clamps
36"
Weight
36"
48"
←12"→
←12"→
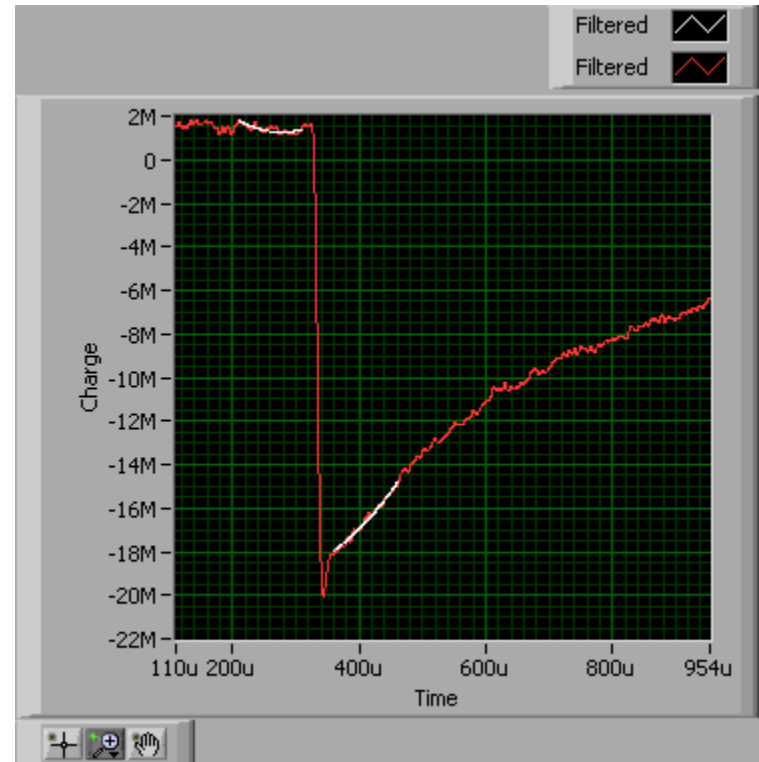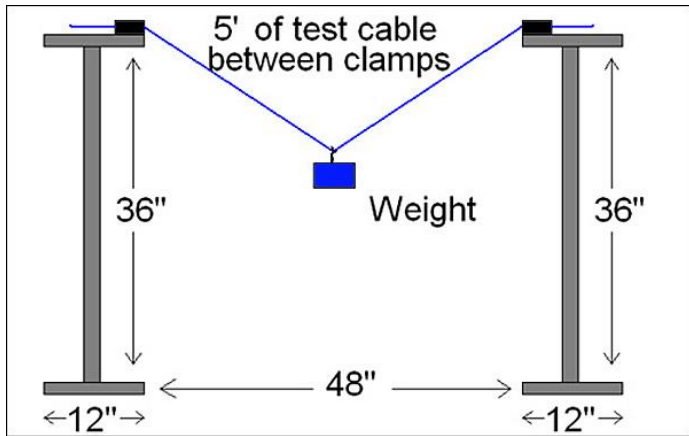
Diagram of triboelectric noise test
set-up specified in ANSI/AAMI 5.5.4 EC53

Weight is 40 times the weight of one foot of cable.
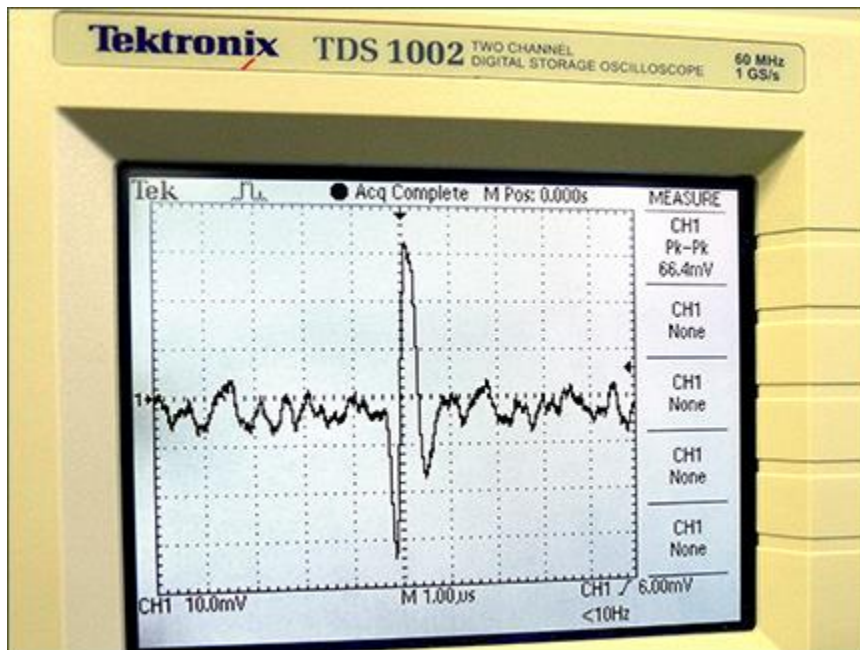
Radial Profile Diagnostic

- Knowing the radius, and more generally the radial profile can be very helpful.
    - Can be used to compute the plasma density. This is critical for studies of waves, 3-body recombination, calculating the collision frequency, etc..
    - Can be used to check for and study instabilities.
    - Can be used to determine basic plasma shape.
    - Will tell you if the charge will fit through subsequent apertures.
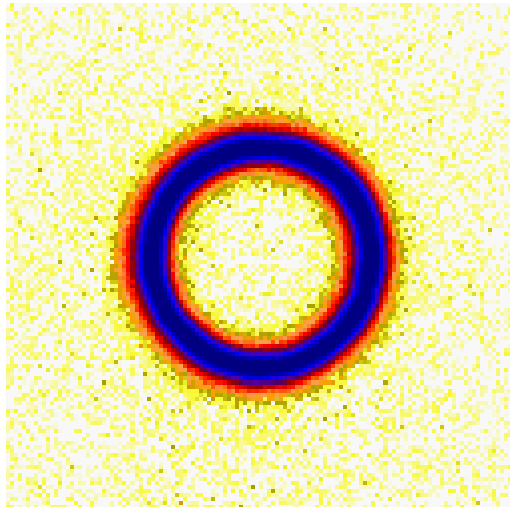
Berkeley
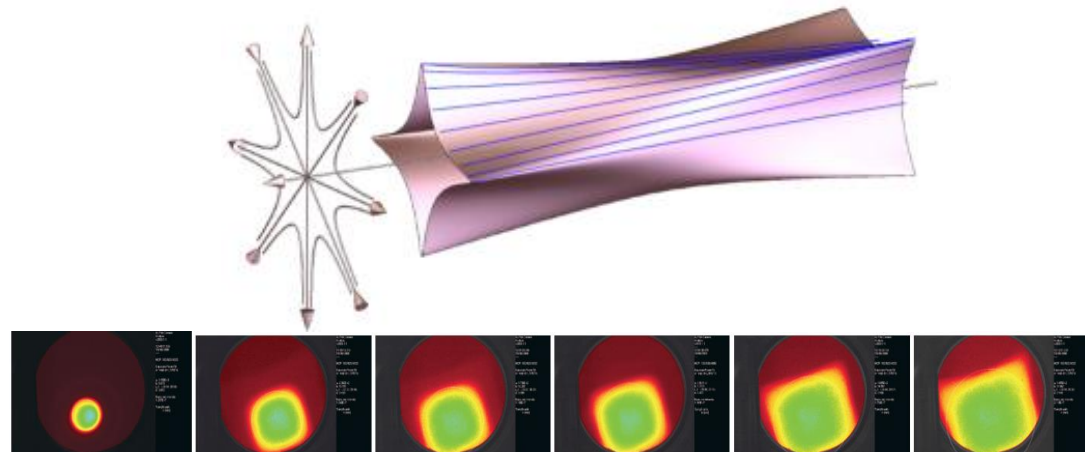
Increasing Octupole Field: ALPHA 2008

Radial Profile

Hollow beam electron gun

Phosphor Screen

Kyhl, R. L.; Webster, H. F., Breakup of hollow cylindrical electron beams, IRE Trans. Electron Dev., **3**, 172 (1956).
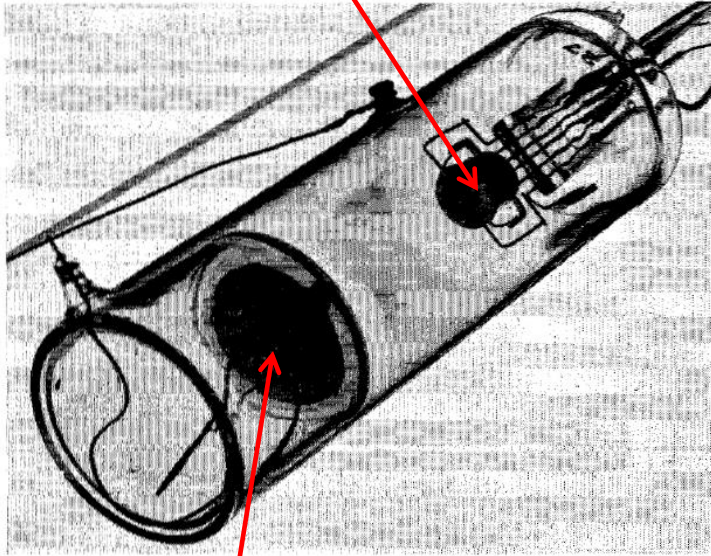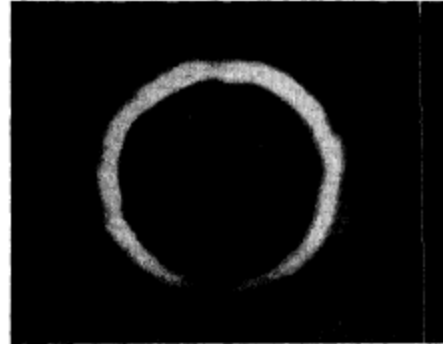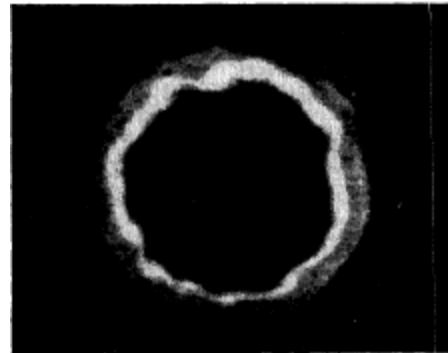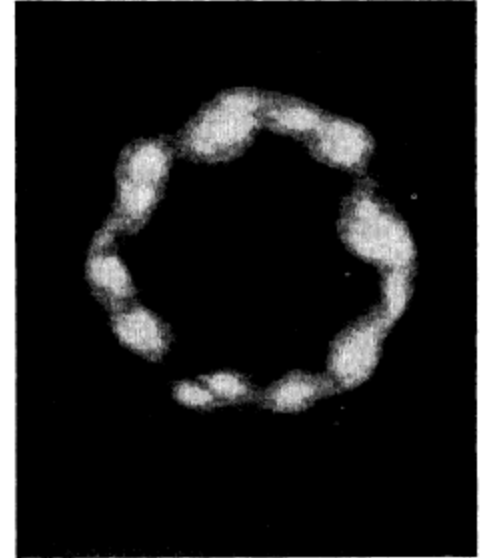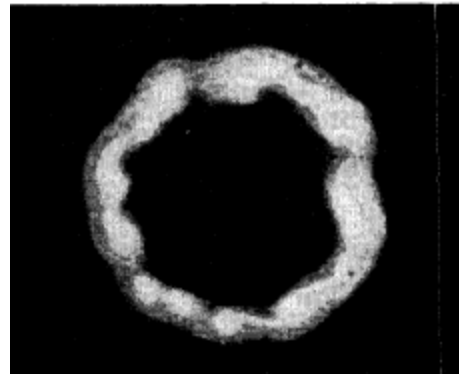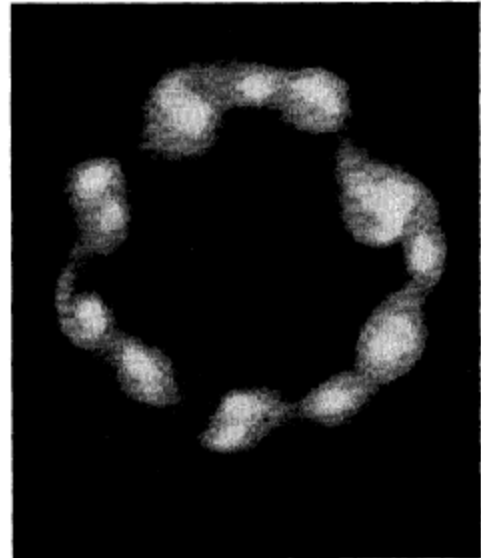
Radial Profile
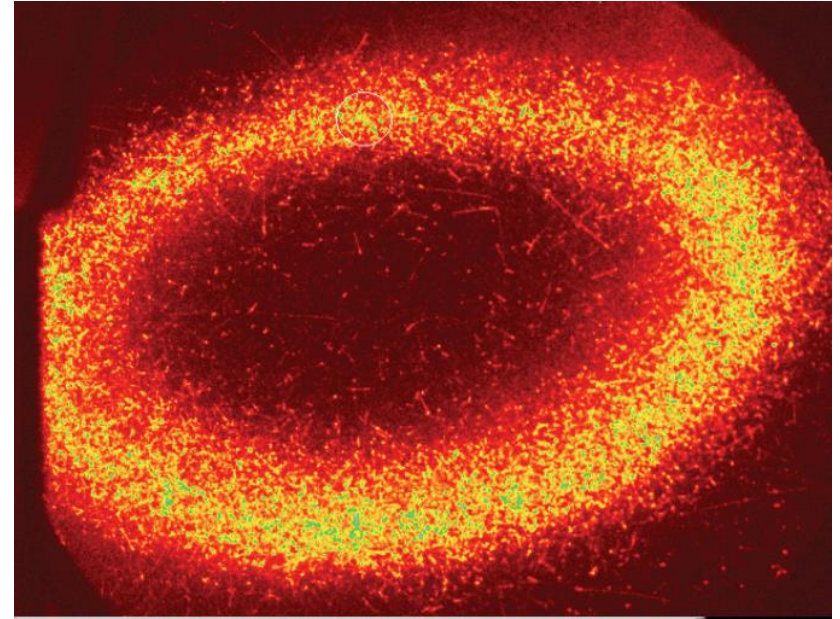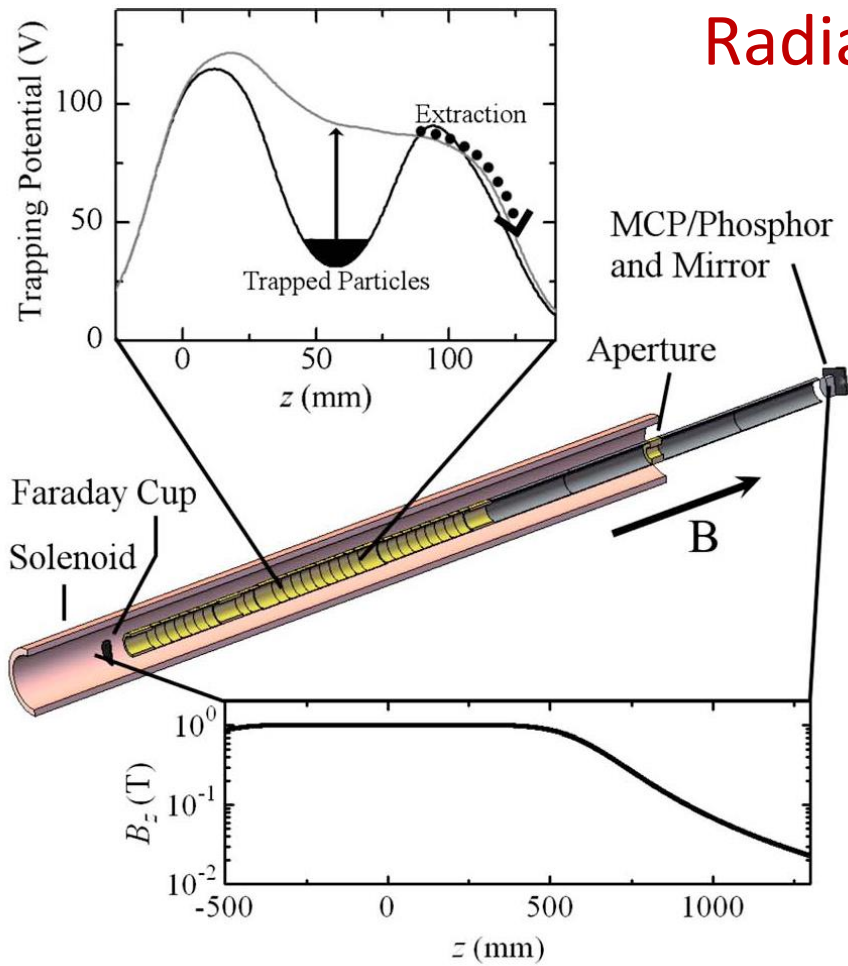
Hollow antiproton plasma imaged on a microchannel plate, ALPHA 2012
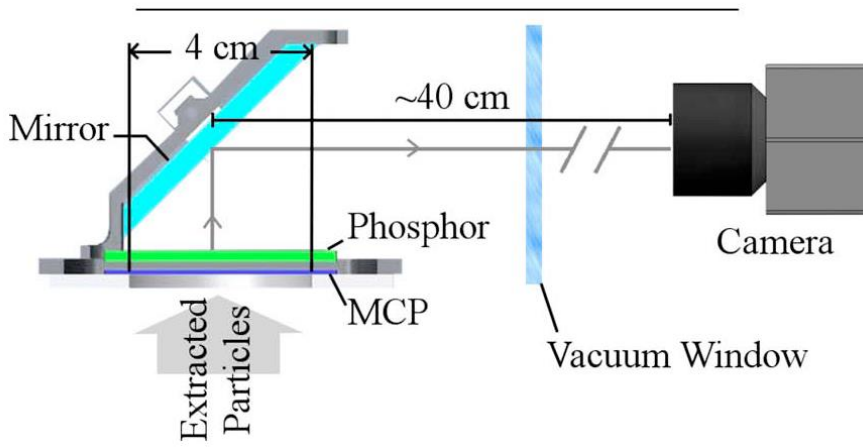
A. J. Peurrung and J. Fajans, A pulsed, microchannel plate-based, non-neutral plasma imaging system. *Rev Sci. Instrum.*, **64**:52, 1993.
G.B. Andresen, et al Antiproton, Positron, and Electron Imaging with a Microchannel Plate/Phosphor Detector, Rev. Sci. Inst., **80**, 123701, 2009.

Phosphor Screens

http://www.beamimaging.com/pscreen.html

Aluminium reflection layer

Phosphor layer

ITO layer

Chromium ring

Substrate

http://www.proxivision.de/products/phosphor-screen.html
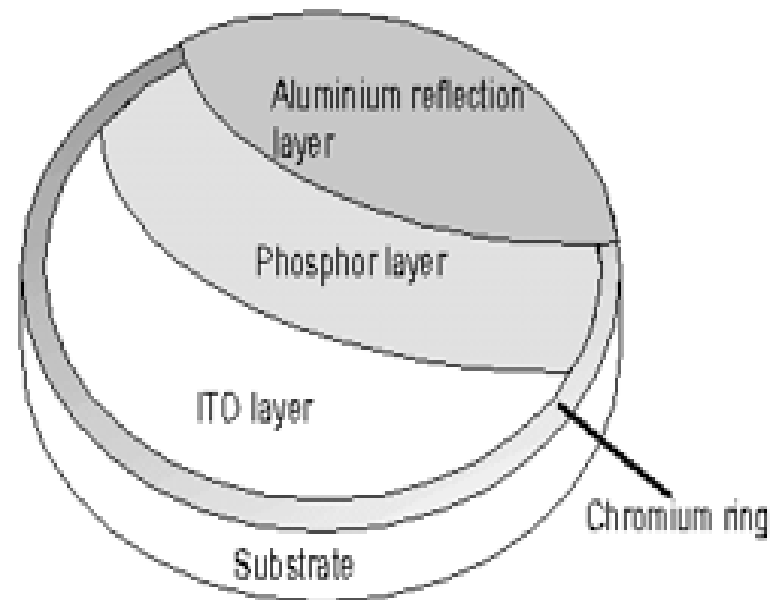
Phosphor Screen

type	composition	emission		decay
P43	$Gd_2O_2S:Tb$	540 nm	green	1 ms
P46	$Y_3Al_5O_{12}:Ce$	530 nm	green	300 ns
P47	$Y_2SiO_5:Ce,Tb$	400 nm	blue	100 ns

Type	efficiency (lm/µA)				efficiency (W/mA)				efficiency (ph/el)			
	6 kV	10 kV	12 kV	15 kV	6 kV	10 kV	12 kV	15 kV	6 kV	10 kV	12 kV	15 kV
P43	0,24	0,43	0,54	0,71	0,43	0,77	0,97	1,28	185	330	420	550
P46	0,08	0,15	0,19	0,25	0,22	0,39	0,49	0,65	90	160	200	265
P47	0,06	0,11	0,14	0,18	0,62	1,35	1,71	2,24	212	380	480	

http://www.proxivision.de/products/phosphor-screen.html

http://www.andor.com/learning-academy/
ccd-spectral-response-%28qe%29-defining-the-qe-of-a-ccd
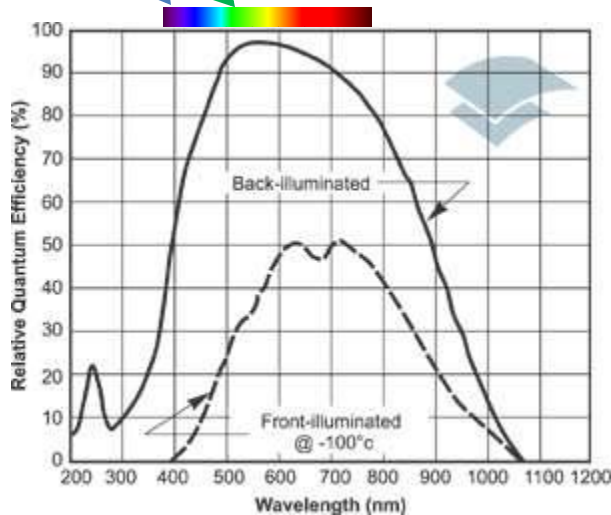
- Detection Efficiency:
    - Phosphor Efficiency.
    - Detector (likely a CCD camera) efficiency.
- Generally, slow phosphors are more efficient.

Phosphor Screen Brightness
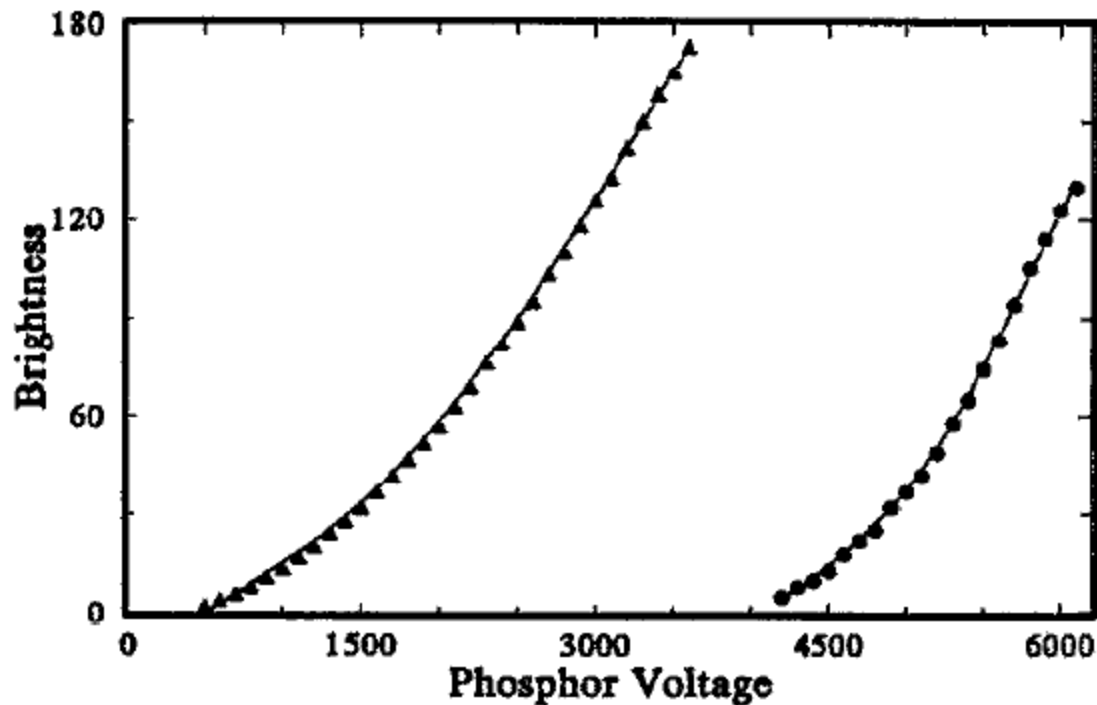
A. J. Peurrung and J. Fajans, A pulsed, microchannel plate-based, non-neutral plasma imaging system. Rev Sci. Instrum., 64:52, 1993.

- Minimum voltage with a screen can be as low as about 1500V.
- Approximately 100 photons per electron is typical.

Microchannel Plates

photonis.com
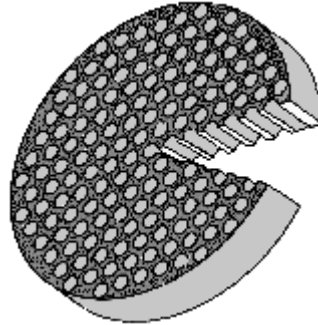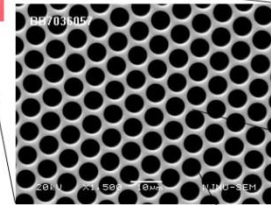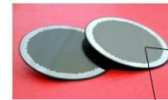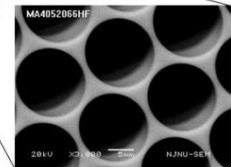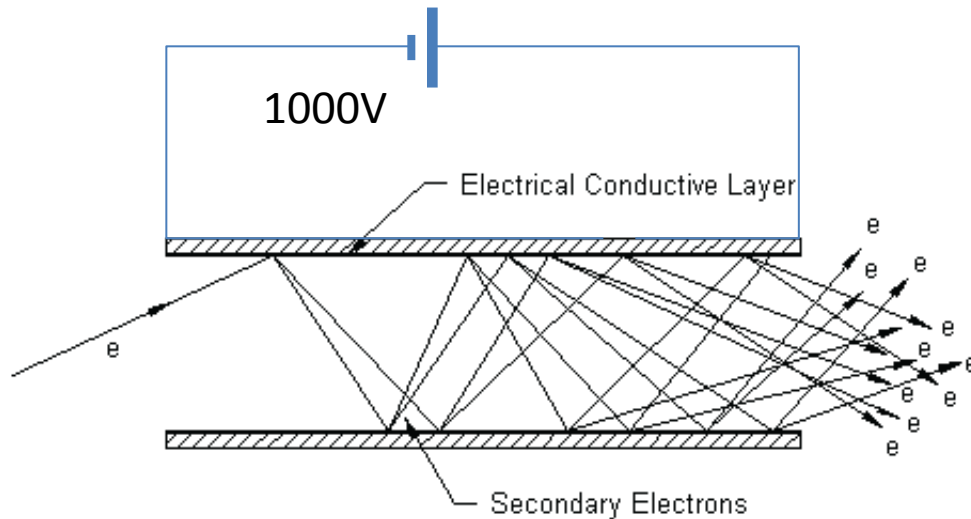
http://www.tectra.de/MCP.htm

http://www.tectra.de/MCP.htm

Typical pore size 2 - 25µm

1000V

Electrical Conductive Layer

e

e
e
e
e
e
e
e
e
e
e
e

Secondary Electrons

http://www.pe1hmm.nl/xx1080/Introduction%20to%20Image%20Intensifier%20Tubes.htm

Microchannel Plate Gain

http://www.optimacorp.co.jp/BurleEO/MCP.htm
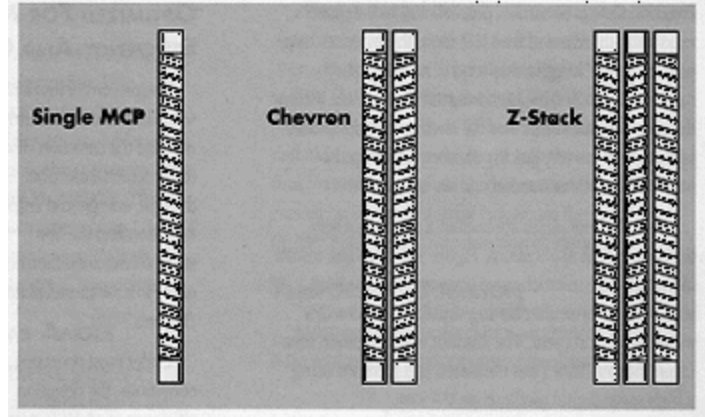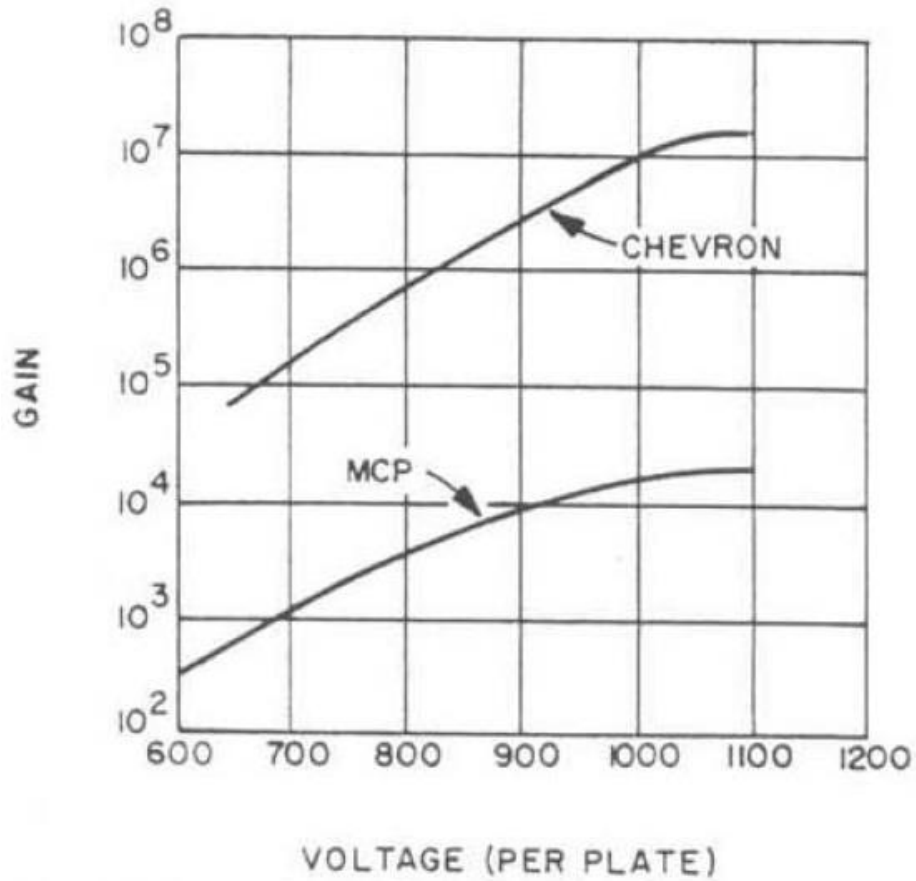
J. Wiza, Microchannel Plate Detectors, Nuclear Instruments and Methods, **162**, 587 (1979).

What limits Microchannel Plate?
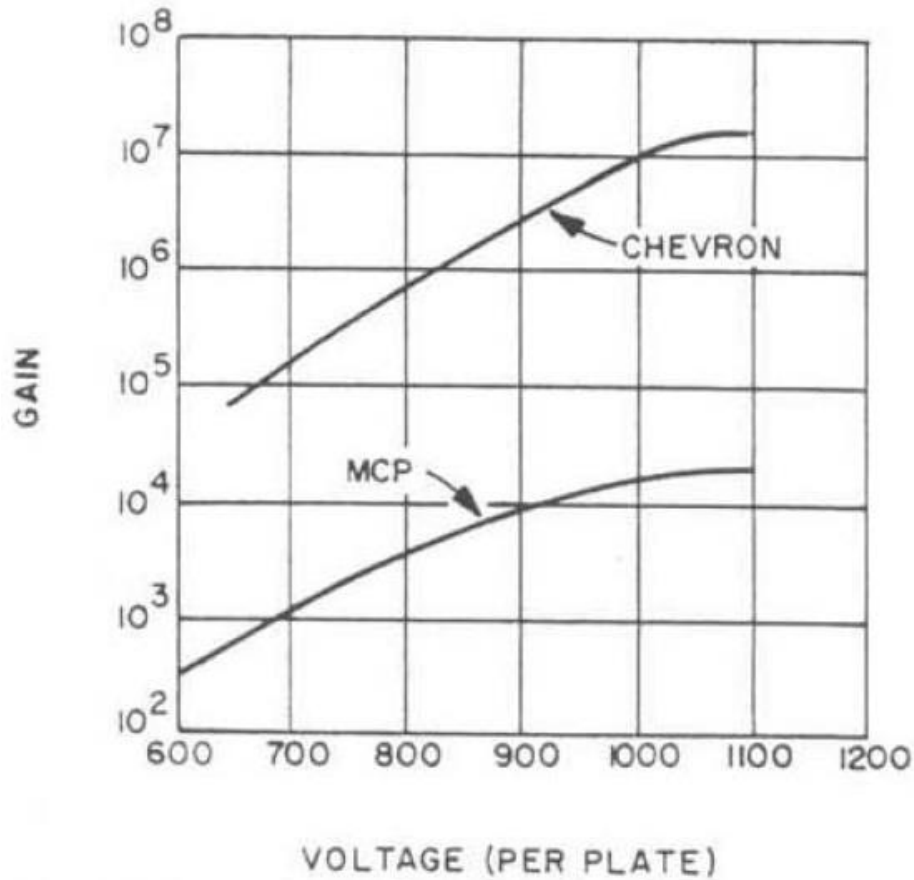
- MCP starts to arc at high voltages.
- Channel get exhausted.

http://www.pe1hmm.nl/xx1080/Introduction%20to %20Image%20Intensifier%20Tubes.htm
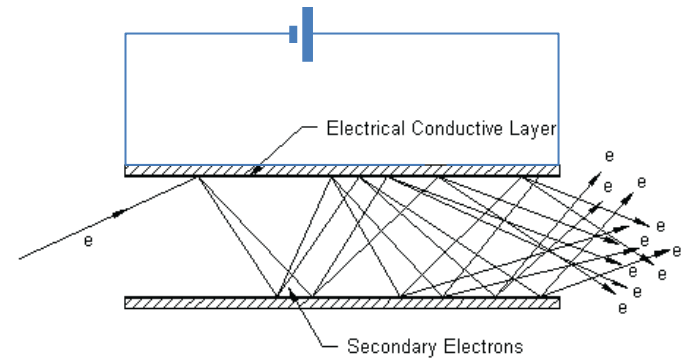
J. Wiza, Microchannel Plate Detectors, Nuclear Instruments and Methods, **162**, 587 (1979).

Microchannel Plate Systems

- MCP Front: Typically between -100 to +100V.
- MCP Back: Typically between 500V to 1200V.
- Phosphor Screen: Typically 3000-10000V.

Photonis APD Detector Brochure

MCP-in electrode
Covering spring foil
MCP-out electrode
Metal anode electrode
Retainer
Metal spacer
MCP
Flange mounting electrode (customer`s dimensions)
Coting
Screen
Foil
Ceramic Insulator
Flange mounting
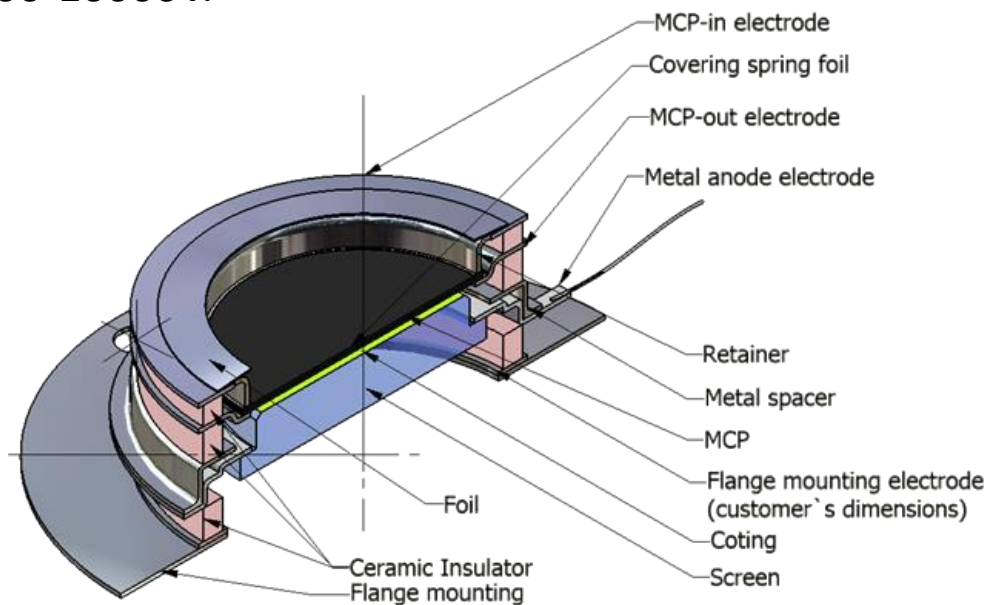
http://www.dmphotonics.com/MCP_MCPImageIntensifiers/microchannel_plates.htm

Don't do this yourself.

Microchannel Plate System Performance

TABLE I: Detection efficiency of channel multipliers[a].

Type of radiation		Detection efficiency (%)
Electrons	0.2 - 2 keV	50-85
	2 - 50 keV	10-60
Positive ions	0.5 - 2 keV	5-85
(H+, He+, A+)	2 - 50 keV	60-85
	50 -200 keV	4-60
U.V. radiation	300 - 1100 Å	5-15
	1100-1500 Å	1-5
Soft X-rays	2 -.50 Å	5-15
Diagnostic X-rays	0.12 - 0.2 Å	~1

[a] From Schagen[17]).

J. Wiza, <u>Microchannel Plate </u>Detectors, Nuclear Instruments and Methods, **162**, 587 (1979).

Coatings available to enhance detection efficiency
For UV and X-rays.

Microchannel Plate System Performance

TABLE I: Detection efficiency of channel multipliers[a].

Type of radiation		Detection efficiency (%)
Electrons	0.2 - 2 keV	50-85
	2 - 50 keV	10-60
Positive ions	0.5 - 2 keV	5-85
(H+, He+, A+)	2 - 50 keV	60-85
	50 -200 keV	4-60
U.V. radiation	300 - 1100 Å	5-15
	1100-1500 Å	1-5
Soft X-rays	2 -.50 Å	5-15
Diagnostic X-rays	0.12 - 0.2 Å	~1

[a] From Schagen[17]).

J. Wiza, Microchannel Plate Detectors, Nuclear Instruments and Methods, **162**, 587 (1979).


Hollow antiproton plasma imaged on a microchannel plate, ALPHA 2012
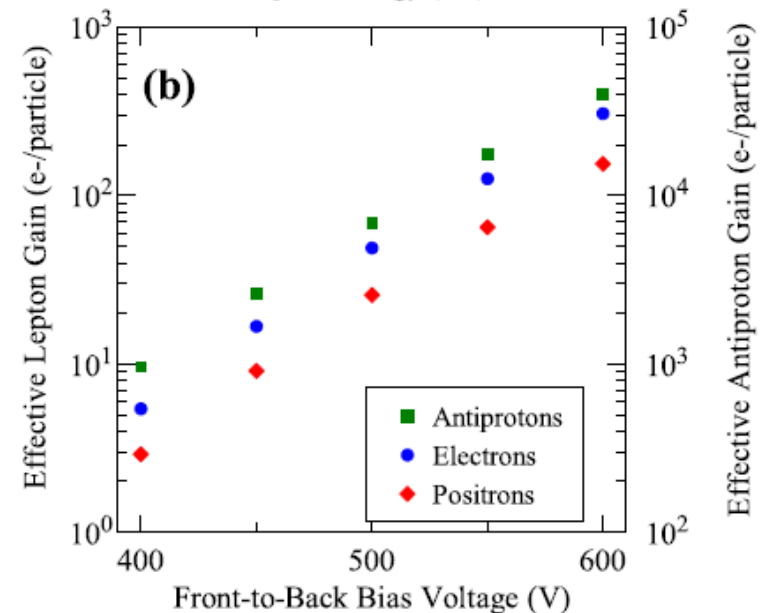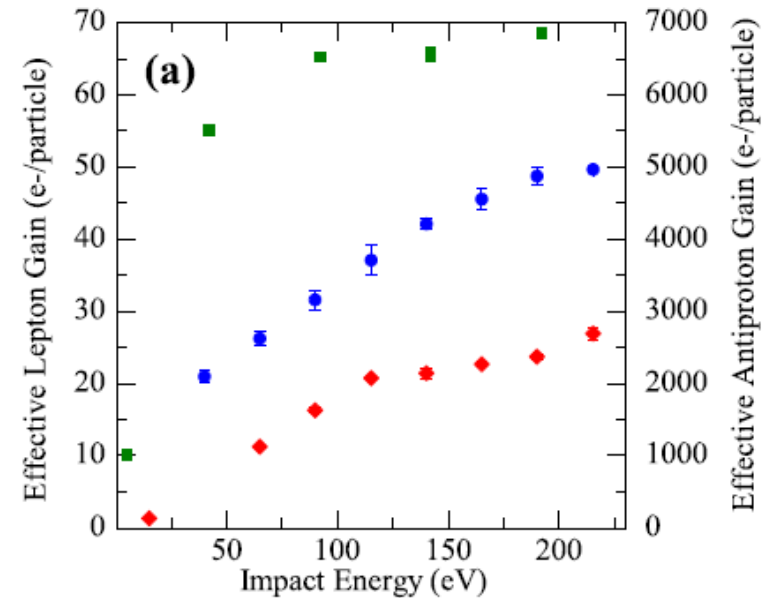
ALPHA, Antiproton, Positron, and Electron Imaging with Microchannel Plate/Phosphor Detector, Rev. Sci. Inst., **80**, 123701, (2009).

Other Radial Diagnostics

- The dream....direct reading of charge onto a CCD-like chip.
  - Electronics would have to be UHV compatible.
  - No opportunity for service.
  - Detector area likely to be small.
 - Possibly complex electrical feedthrough issues.
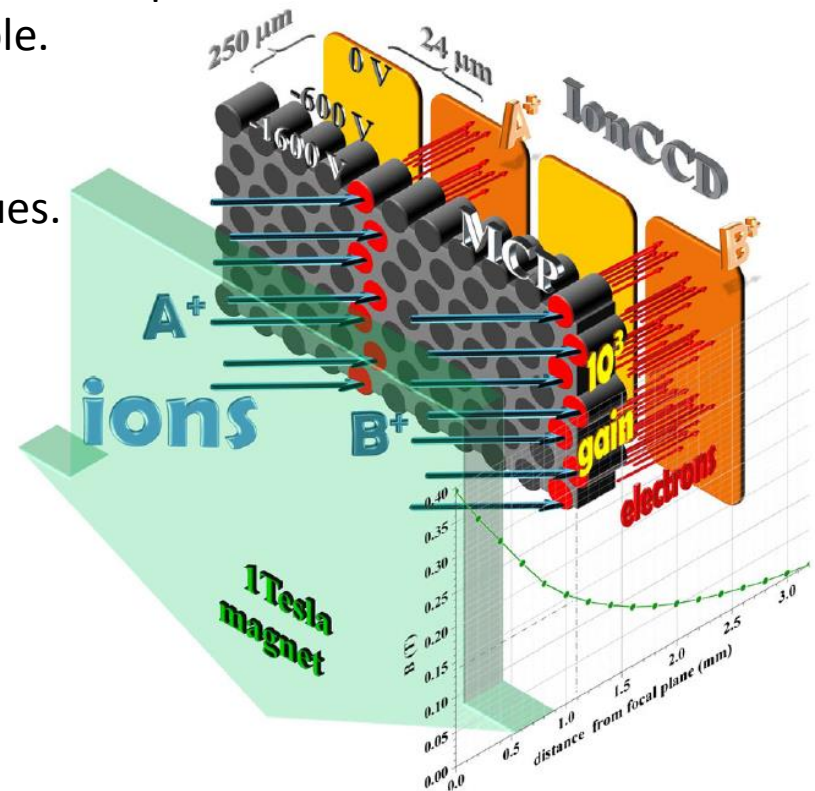
O. Hadjar, W.K. Fowler, G. Kibelka, W.C. Schnute, Preliminary demonstration of an IonCCD as an alternative pixelated anode for direct MCP readout in a compact MS-based detector, J. Am. Soc. Mass. Spectrom., **23**, 418, (2012).

Other Radial Diagnostics

- Multiple ring Faraday cups and possibly expansion by magnetic field reduction.
  - Very crude.
  - Very slow if magnetic expansion is used. Plasma may change during expansion.
  - Usually requires many trials.
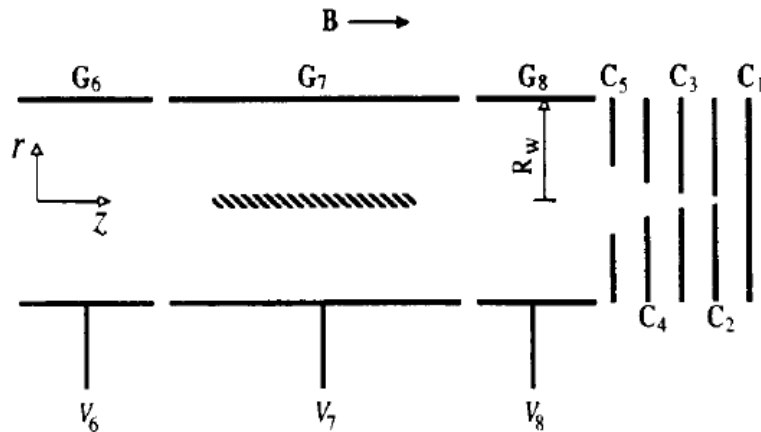

B. R. Beck, J. Fajans and J. H Malmberg, Temperature and anisotropic-temperature relaxation measurements in cold, pure-electron plasmas. *Phys. Plasmas*, **3**:1250, 1996.
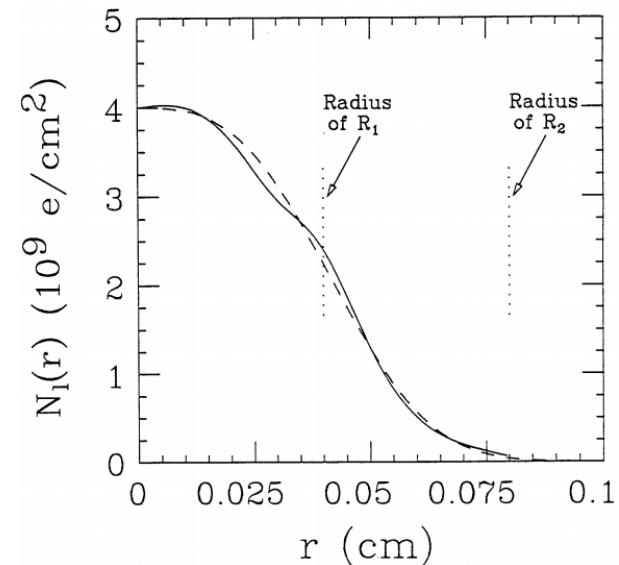
B.R. Beck, Measurement of the magnetic and temperature dependence of the electron-electron anisotropic temperature relaxation rate., Ph.D. Thesis, UCSD (1990).

Other Radial Diagnostics

- Magnetic field lowering and antiproton annihilation.
  - Very crude.
  - Plasma may change during expansion.

- Total Charge and Inner Line Density Faraday Cups
  - Requires the assumption of global thermal equilibrium.
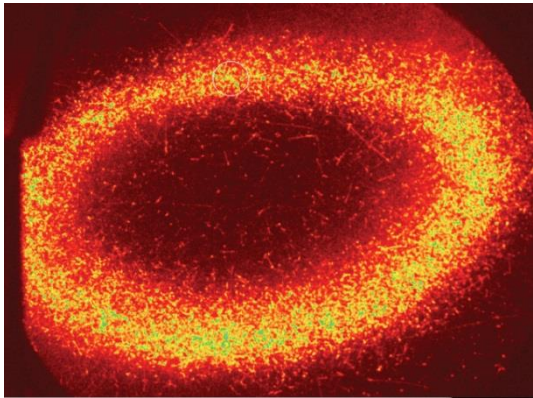
Hollow antiproton plasma imaged on a microchannel plate,
ALPHA 2012

Berkeley

Berkeley

G. Gabrielse et al, Centrifugal separation of antiprotons and electrons, Phys. Rev. Lett., **105**, 213002, (2010).

P. Oxley et al, Aperture method to determine the density and geometry of anti-particle plasmas, Phys. Lett. B **595**, 60 (2004).
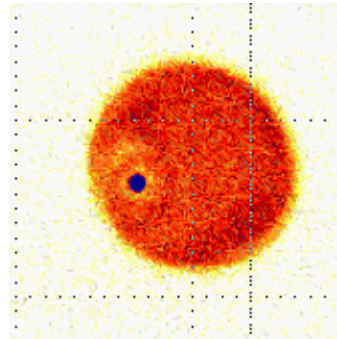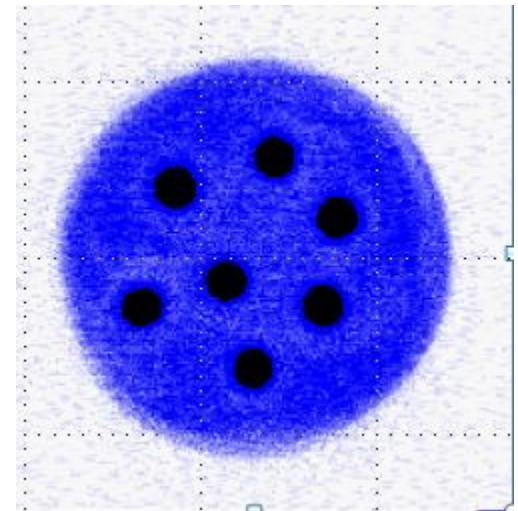
Density Reconstruction

- There are methods to measure the density directly, but frequently the density is inferred from:
  - Measurements of the total charge.
  - Measurements of the radial profile.
  - Measurement (or assumption) of the plasma temperature.
  - Knowledge of the potentials on the electrodes.
- Algorithm:
  - Assume local thermal equilibrium along magnetic field lines. Then simultaneously solve:
    - Poisson's equation: $\epsilon_0 \nabla^2 \Phi(r, z) = en(r, z)$, where $n(r, z)$ is the local density, and e is the unit charge.
    - Boltzmann's equation at every radius:
    $$n(z; r) = n_0(r) exp\left[\frac{-e}{k_B T} \Phi(r, z)\right].$$
    - A normalization condition: $N(r) = \int_{-\infty}^{\infty} n(z; r)dz.$
    - Note that $N(r)$ is itself normalized so that $2\pi \int N(r)rdr$ is the total charge.

Density Reconstruction

- Procedure:
    - From an image of the plasma, construct the radial profile (generally, solvers assume azimuthal symmetry).
    - Then solve the set of equations iteratively.
        - Finite temperature method.   Begin by gridding the trap in (r, z).
            1. Solve Poisson's equation for $\Phi(r, z)$ by Fourier transforming at every r. This yields a set of sparsely coupled equations indexed by r, which can be inverted.
                - Even though one uses an FFT, this is the time consuming step.
            2. Then use $\Phi(r, z)$ to calculate an new "trial" guess for $\hat{n}(z; r)$ at every radius.
            3. Calculate the final new guess $n_{k+1} = (1 - \epsilon)n_k + \epsilon \, \hat{n}(z; r)$. Adjust ε to optimize convergence.
            4. Iterate steps 1-2-3 until the desired convergence is obtained.
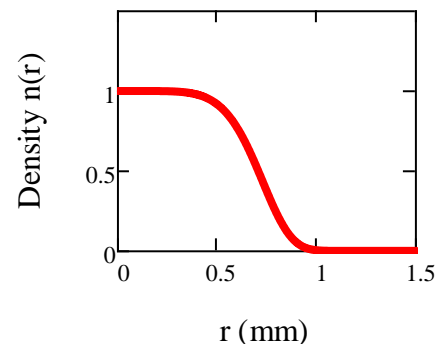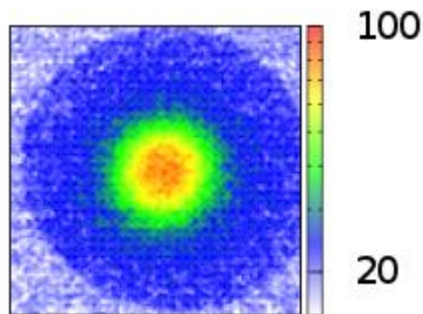
Density Reconstruction

- Procedure:
  - From an image of the plasma, construct the radial profile (generally, solvers assume azimuthal symmetry).
  - Then solve the set of equations iteratively.
    - Finite temperature method. Begin by gridding the trap in (r, z).
    - Convergence is slow.
      - The grid size must be well less than λ_D in z for convergence, and again well less than λ_D to properly model the radial edge.
      - Convergence is particularly slow at low temperatures because λ_D becomes small, and the solutions oscillate if the grid is too crude. But making the grid fine makes the algorithm slow.
        - The practical lower limit is a few hundred Kelvin.
      - If the plasma is not well confined, i.e. if it is near to leaking out over the potential barrier, convergence is also difficult.
      - Typical solve times range from 30s to a few hours…to never.

Density Reconstruction

- Procedure:
  - From an image of the plasma, construct the radial profile (generally, solvers assume azimuthal symmetry).
  - Then solve the set of equations iteratively.
    - Finite temperature method.   Begin by gridding the trap in (r, z).
    - Zero temperatures method.
      - By assuming a "waterbag" model, it is possible to solve this system at $T = 0$.
        - A waterbag is like a plasma filled balloon, with constant density along field lines inside, and zero density outside.
      - With a waterbag, Poisson's equation need only be solved at the waterbag boundary. No need to grid.
      - Convergence is much faster…a few seconds to minutes.

Density Reconstruction

Waterbag example: a barely confined plasma.
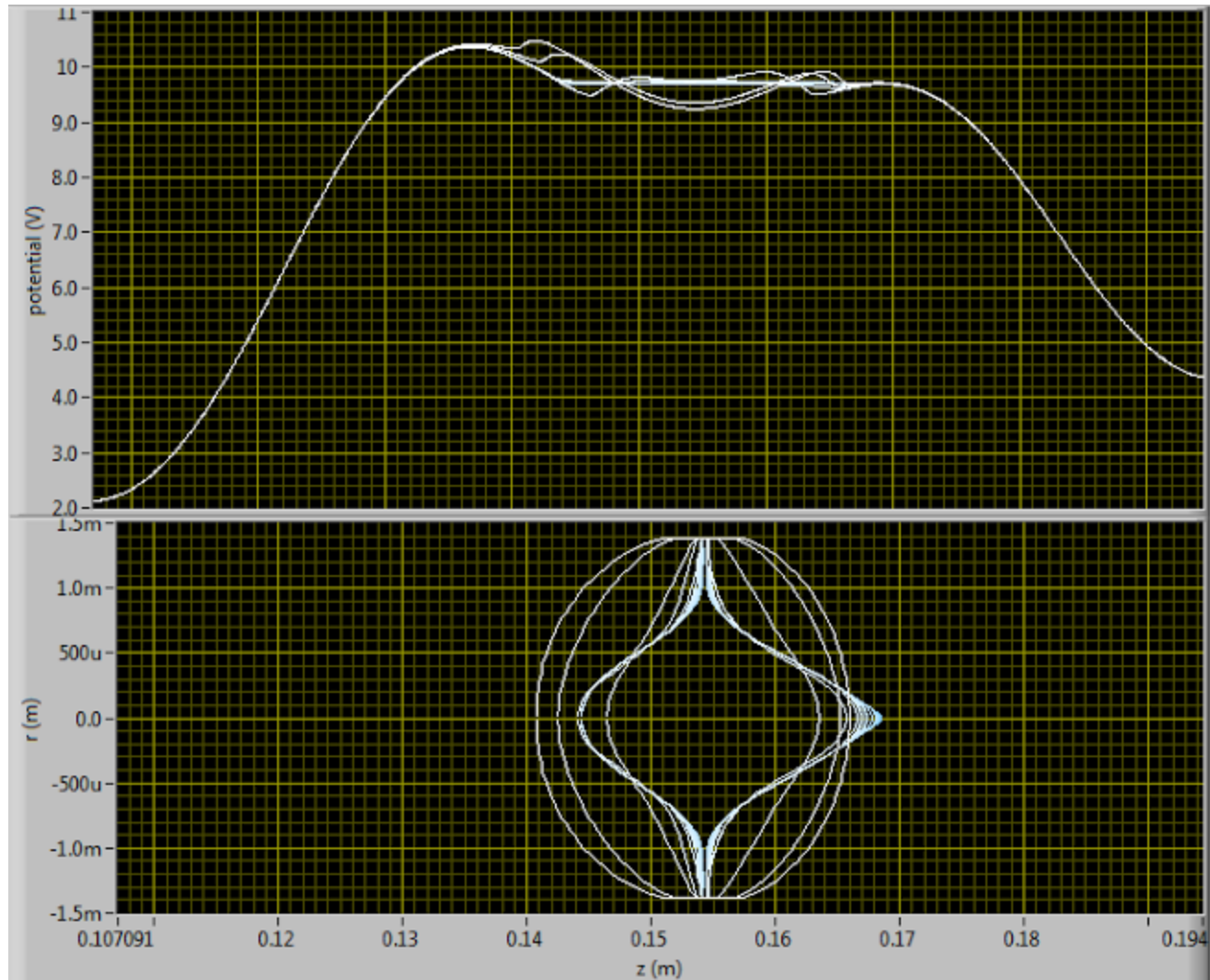
Temperature Diagnostic

- Consider a non-interacting, finite temperature, charged gas held in a potential well.
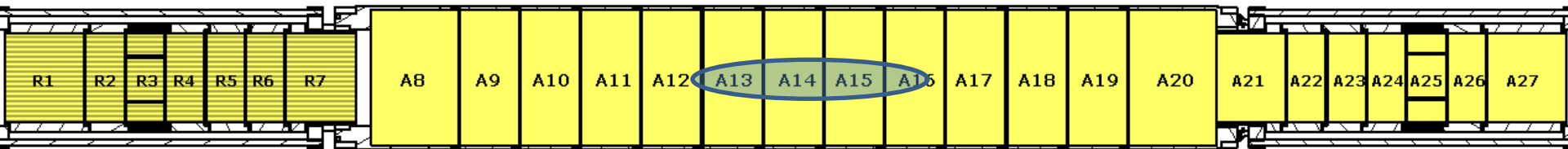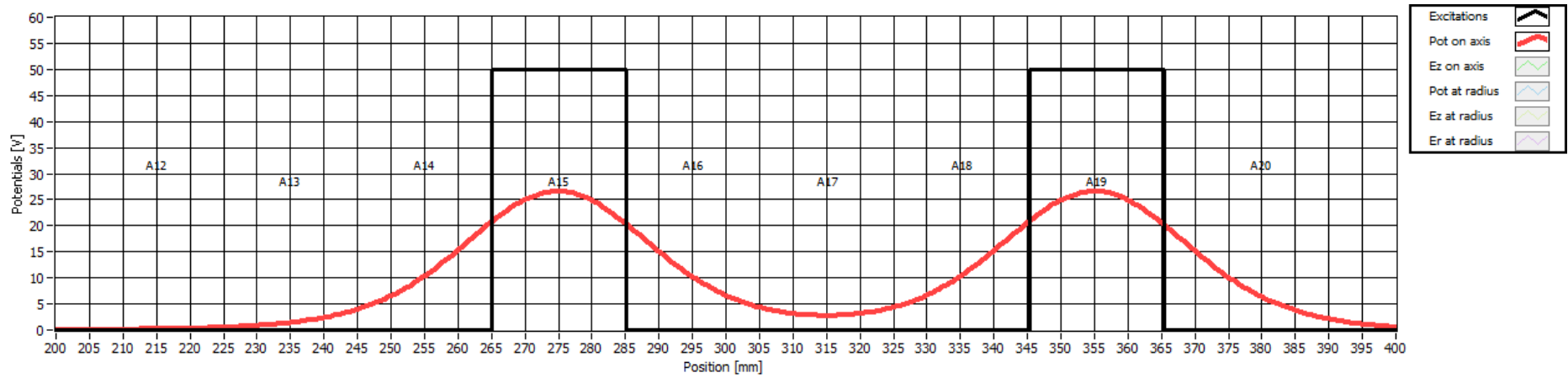
Temperature Diagnostic: Noninteracting Gas

- Consider a noninteracting charged gas held in a potential well.
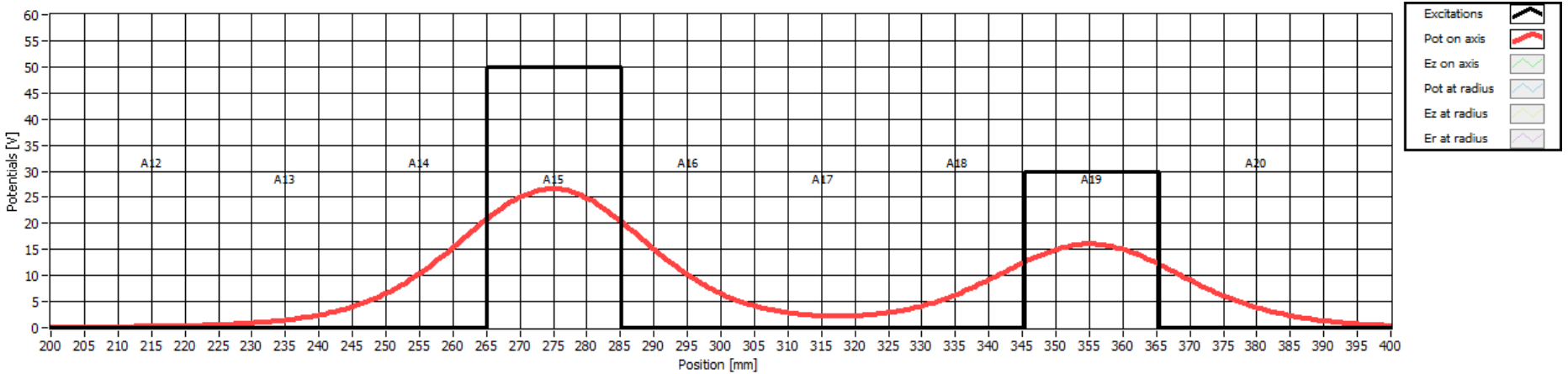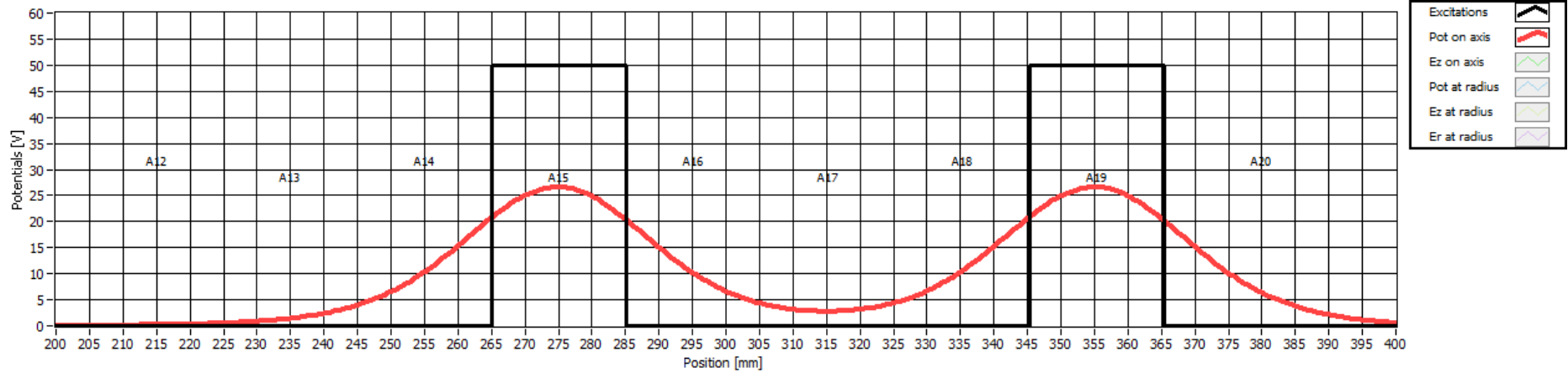
How many gas particles escape?

Temperature Diagnostic: Noninteracting Gas

- Assume the particles in the gas are Maxwellian distributed.
  - Distribution function:
  $$f(E) = \frac{1}{\sqrt{\pi k_B T}} \frac{1}{\sqrt{E}} \exp\left[-\frac{E}{k_B T}\right].$$
- Lower the barrier height to some level $V = e\Phi$.
  - Then the charge that can escape over the barrier is
  $$Q(V) = \frac{1}{\sqrt{\pi k_B T}} \int_V^\infty \frac{1}{\sqrt{E}} \exp\left[-\frac{E}{k_B T}\right].$$
    - This is a complementary error function.
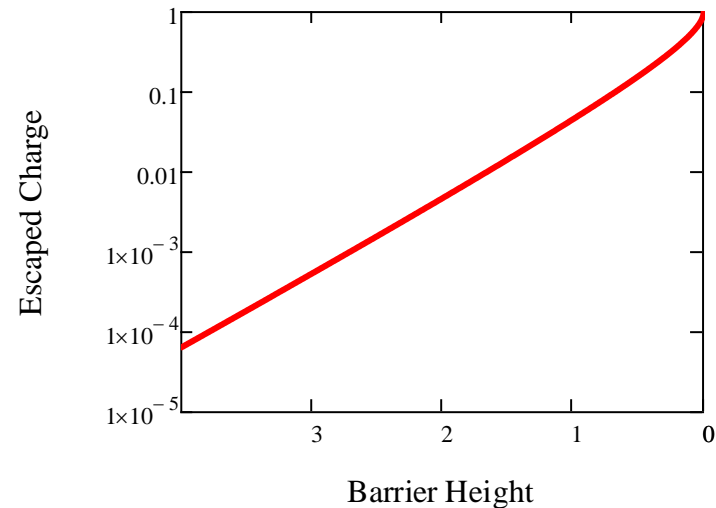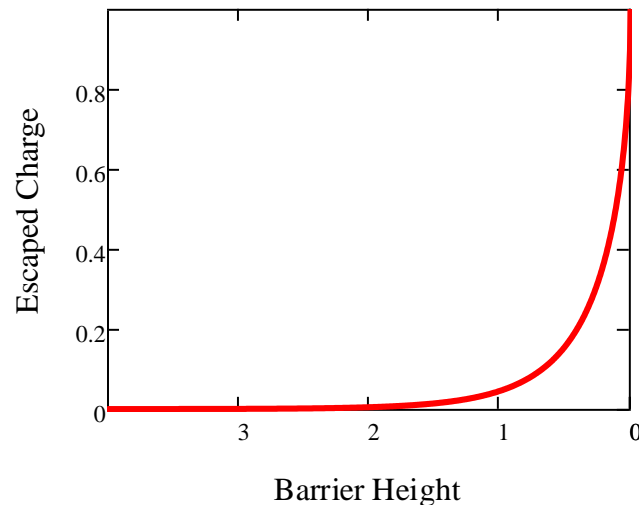
- What is the slope on the log graph?

- Starting with:

$$Q(V) = \frac{1}{\sqrt{\pi k_B T}} \int_V^\infty \frac{1}{\sqrt{E}} \exp\left[-\frac{E}{k_B T}\right].$$

- We want to calculate

$$\frac{d \ln(Q(V))}{dV} = \frac{1}{Q(V)} \frac{d(Q(V))}{dV}.$$

- Taking the derivative, we get:

$$\frac{\frac{1}{\sqrt{V}} \exp\left[-\frac{V}{k_B T}\right]}{\int_V^\infty \frac{1}{\sqrt{E}} \exp\left[-\frac{E}{k_B T}\right]}$$

- This can be rewritten as:

$$\frac{\frac{1}{\sqrt{V}} \exp\left[-\frac{V}{k_B T}\right]}{\exp\left[-\frac{V}{k_B T}\right] \int_0^\infty \frac{1}{\sqrt{E+V}} \exp\left[-\frac{E}{k_B T}\right]} = \frac{\frac{1}{\sqrt{V}}}{\int_0^\infty \frac{1}{\sqrt{E+V}} \exp\left[-\frac{E}{k_B T}\right]}$$

Temperature Diagnostic: Noninteracting Gas

- This can be further simplified as:

$$\frac{\dfrac{1}{\sqrt{V}}}{\int_0^\infty \dfrac{1}{\sqrt{E+V}} \exp\left[-\dfrac{E}{k_B T}\right]} = \frac{1}{\int_0^\infty \dfrac{1}{\sqrt{1+E/V}} \exp\left[-\dfrac{E}{k_B T}\right]}$$

- When we are reasonably far out on the tail, $E \ll V$, so we can approximate the above expression to:

$$\frac{1}{\int_0^\infty \exp\left[-\dfrac{E}{k_B T}\right]} = -\frac{1}{k_B T}$$

- Therefore, the slope of the log of the escaped charge is inversely proportional to the temperature.

- A better approximation yields:

$$\frac{d\ln(Q)}{dV} = \frac{-1.05}{k_B T}$$
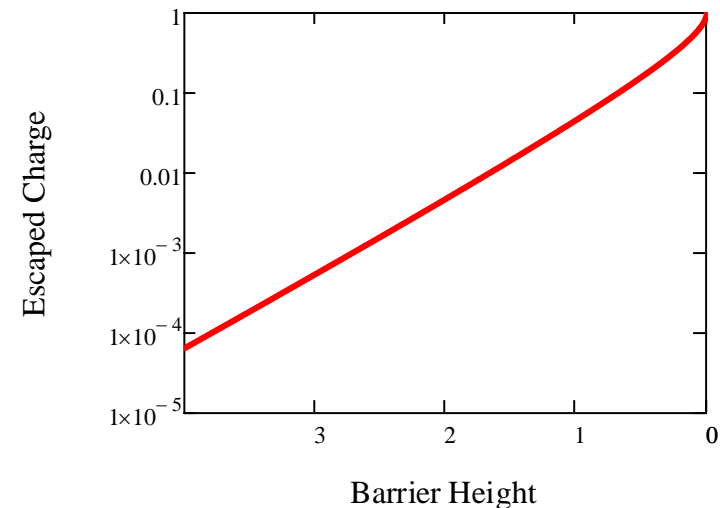
# Temperature Diagnostic: Simple Complication
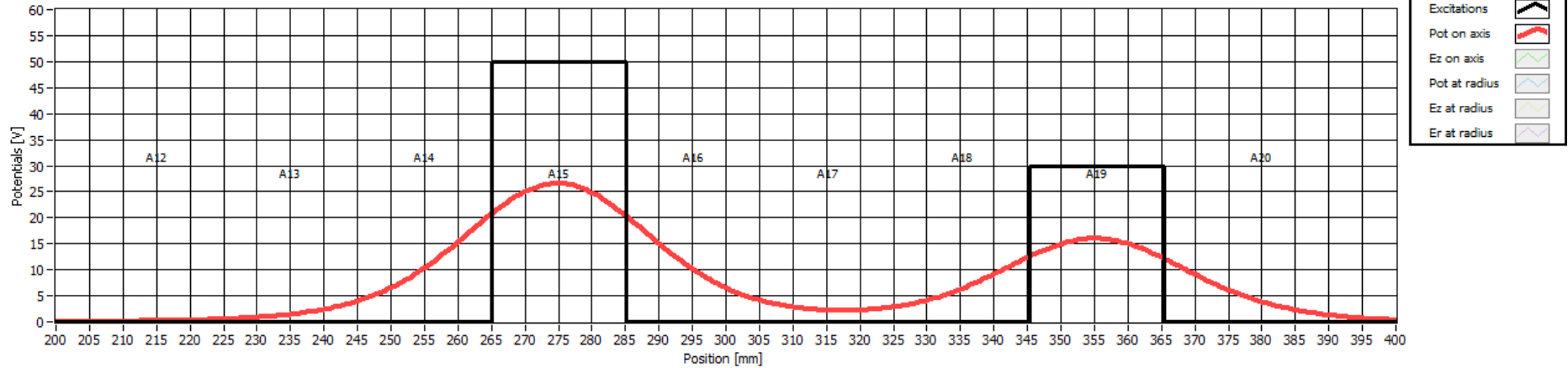
- The wall potential is not the well potential:
  - The on-axis potential maximum is typically about 50% of the wall potential.
    - The exact ratio depends on the electrode radius to length radius.
  - The potential in the middle of the trap is not zero.
- Both these effect need to be accounted for in the voltage derivative.
- These issues are increasingly important in short traps.
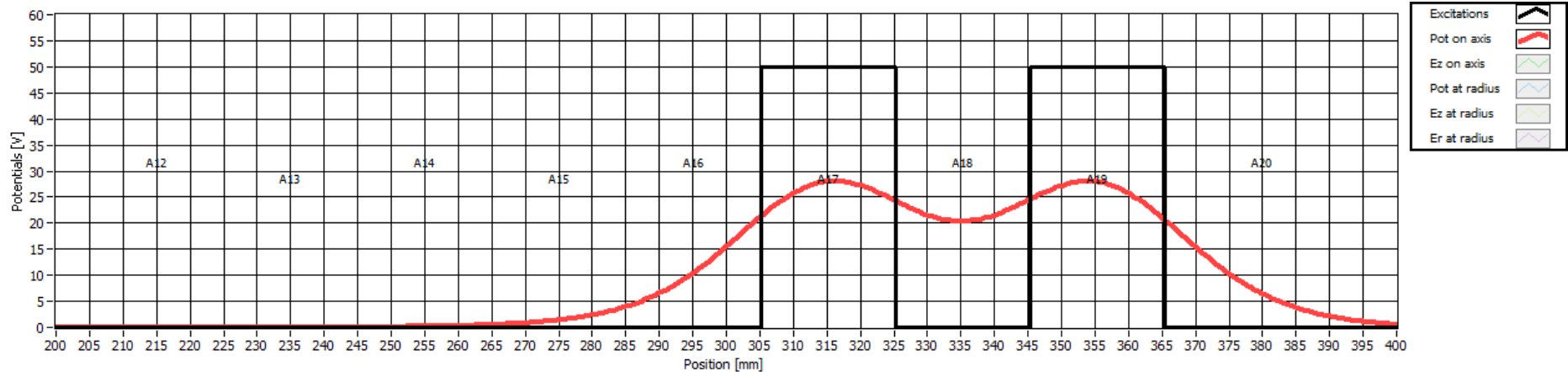
Temperature Diagnostic: Modest Complication
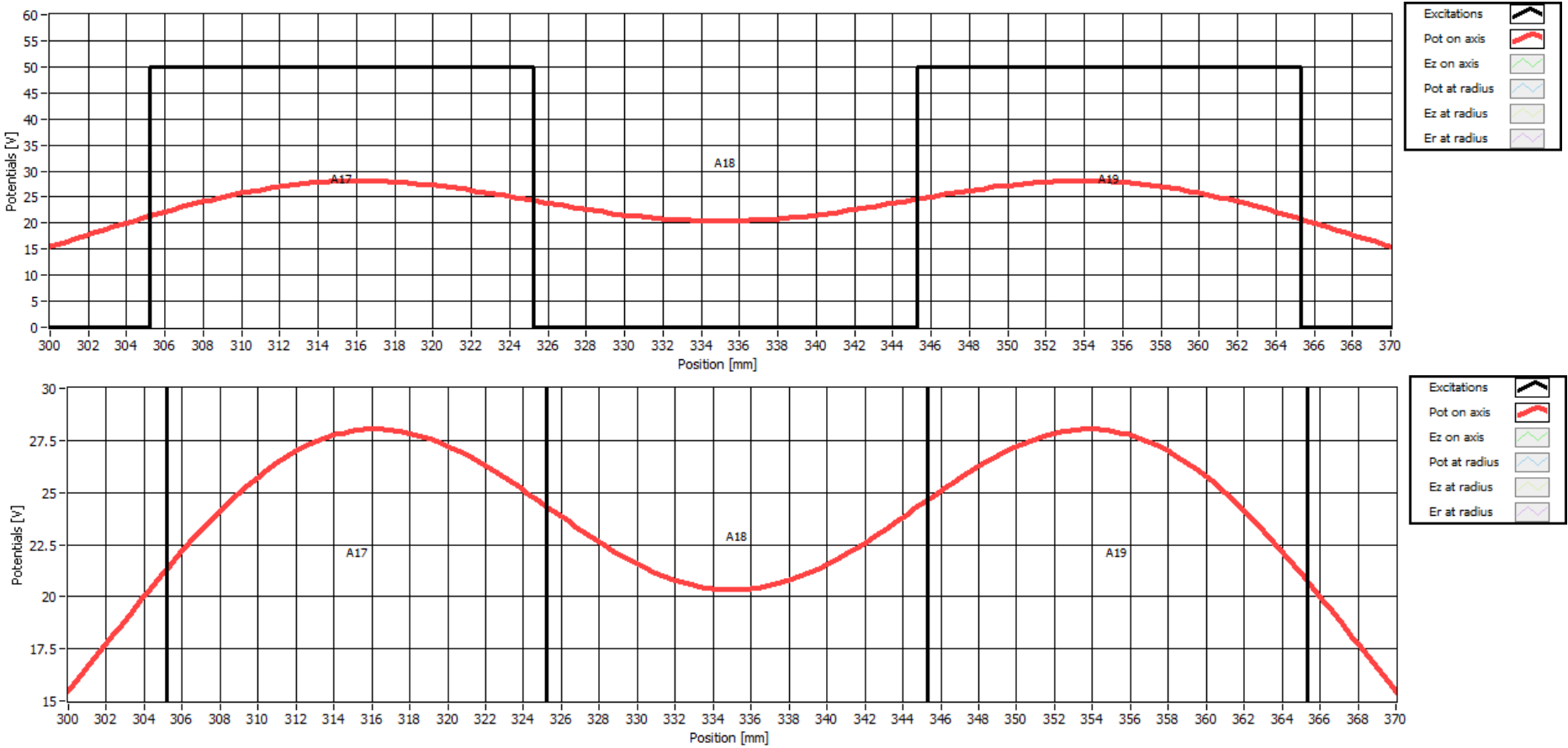
Temperature Diagnostic: Modest Complication
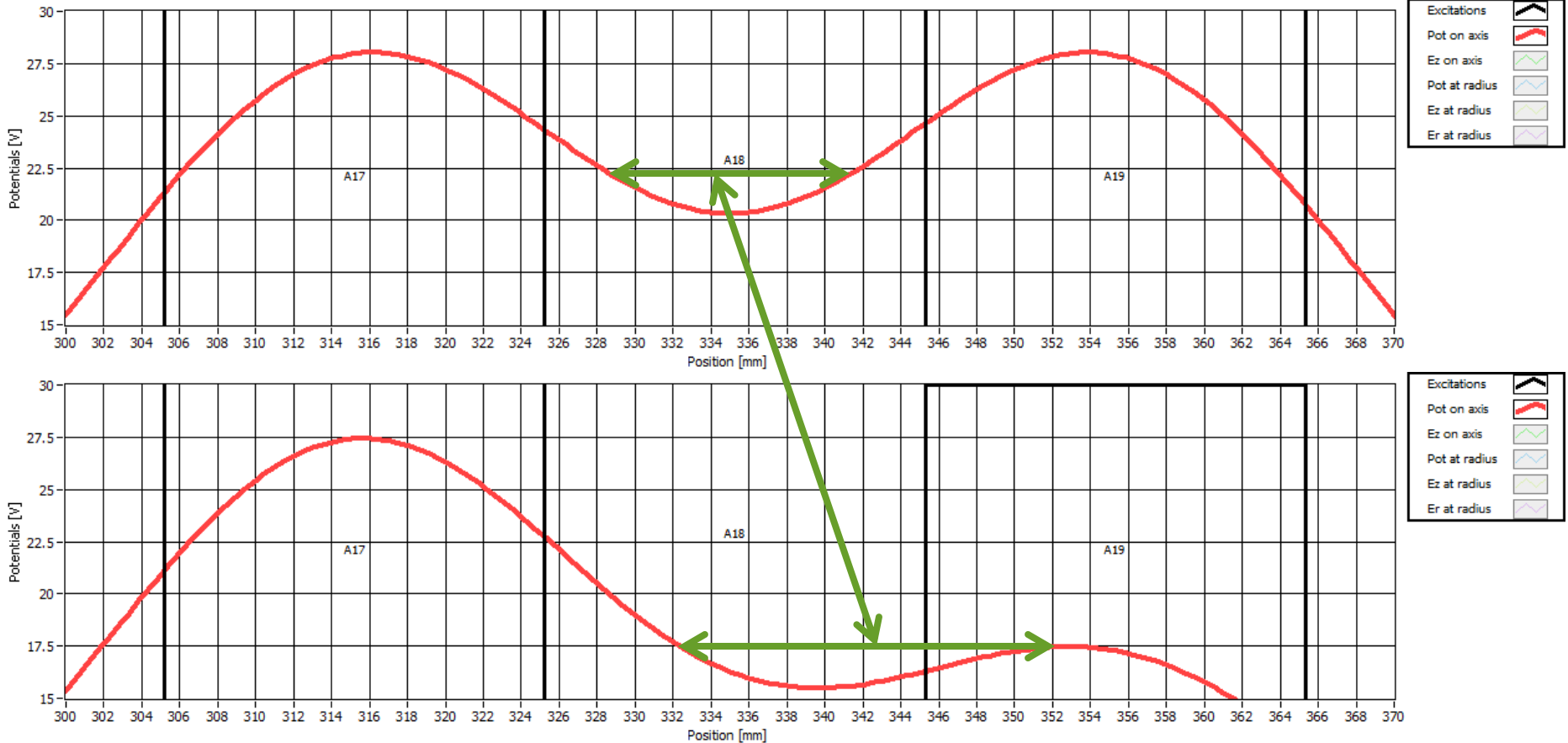
- Plasma expands during release.
  - 1D adiabatic expansion: temperature declines to 41% of its original value in this example.
  - Plasma may undergo 3D expansion: temperature declines to 74% of its original value in this example.
  - Actual expansion may be between 1D and 3D.

Temperature Diagnostic: Collective Effects

- The self field of a plasma severely complicates the theoretical description of this diagnostic.
  - The potential of a solid infinite cylinder is

$$\Phi(r) = \frac{en_0}{4\epsilon_0} R^2 \left[1 - \frac{r^2}{R^2} + 2\ln\left(\frac{R_W}{R}\right) \right],$$

  inside the plasma, and

$$\Phi(r) = \frac{en_0}{2\epsilon_0} R^2 \ln\left(\frac{R_W}{R}\right),$$

  outside the plasma, where n_0 is the density, R is the plasma radius and R_W is the electrode wall radius.
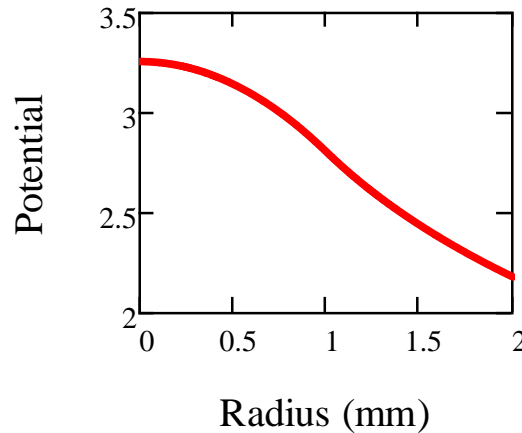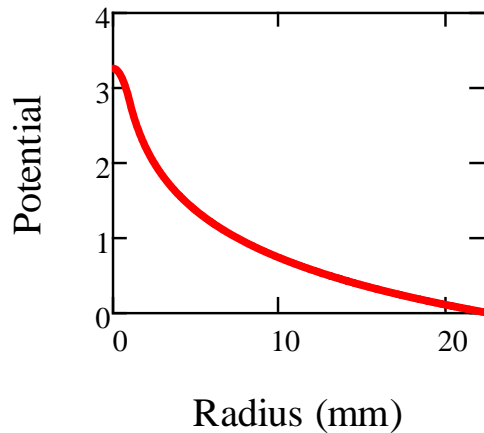

Typical alpha parameters:
$$n_0 = 10^8 \text{ cm}^{-3}$$
$$R = 1\text{mm}$$
$$R_W = 22.28\text{mm}$$

- The self potential is largest on the axis.

# Temperature Diagnostic: Radial Effects
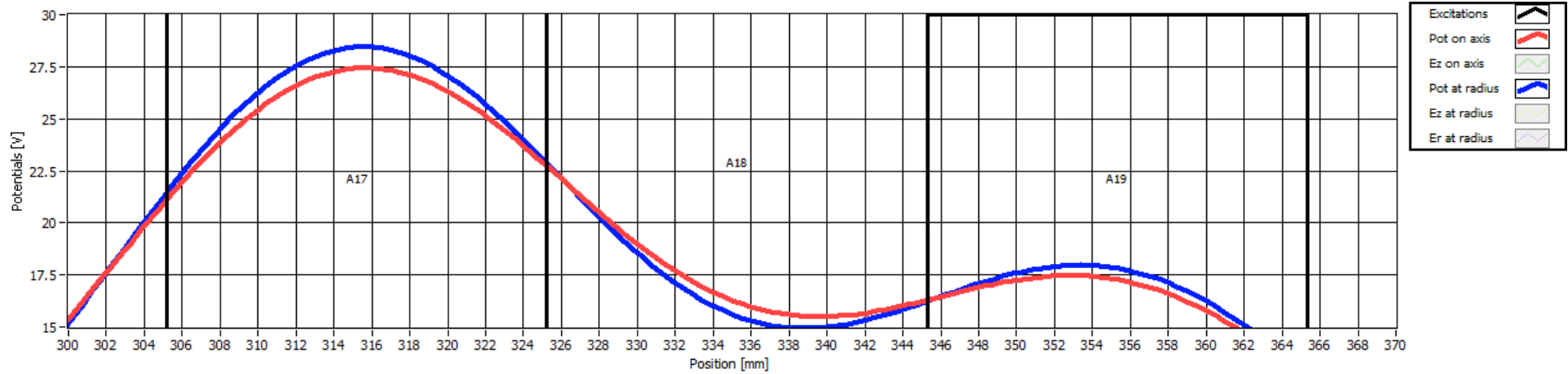

Well is deeper off-axis.
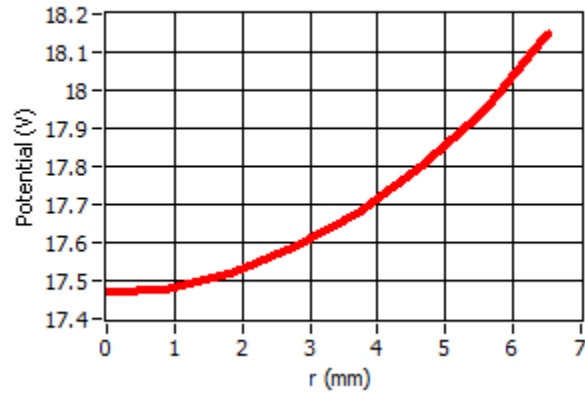
Temperature Diagnostic: Collective Effects
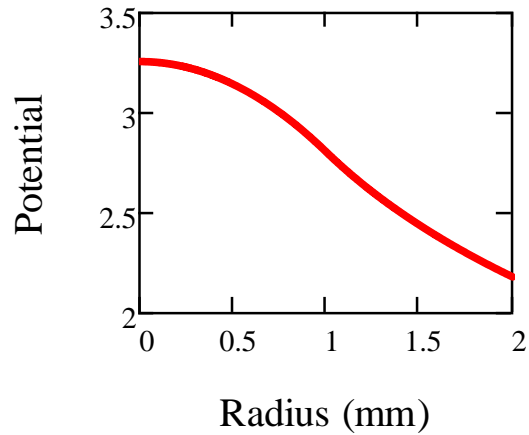
The self potential is largest on the axis.
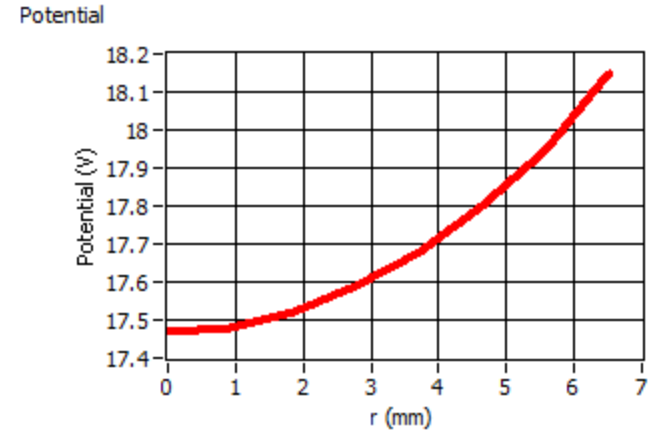

Well is deeper off-axis.

Both these effects lead to the plasma escaping on the axis first.

Temperature Diagnostic: From Where Does the Plasma Escape?

- Initially, the plasma escapes from a central region on the order of several Debye lengths:

$$\lambda_D = \sqrt{\frac{\epsilon_0 k_B T}{n_0 e^2}}$$

- Eventually, the center erodes significantly.
- Once this happens, many things go wrong.
  - Nontail particle begin to escape. The diagnostic was predicated on only tail particles escaping.
  - The plasma hollows out, and the plasma potential changes significantly.
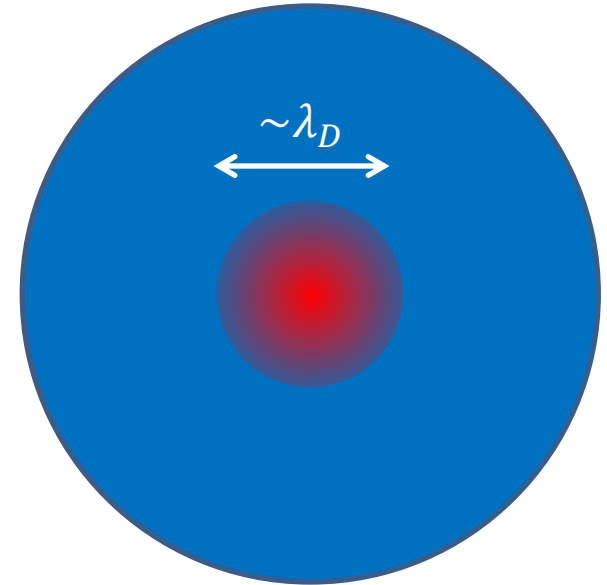
Plasma End View
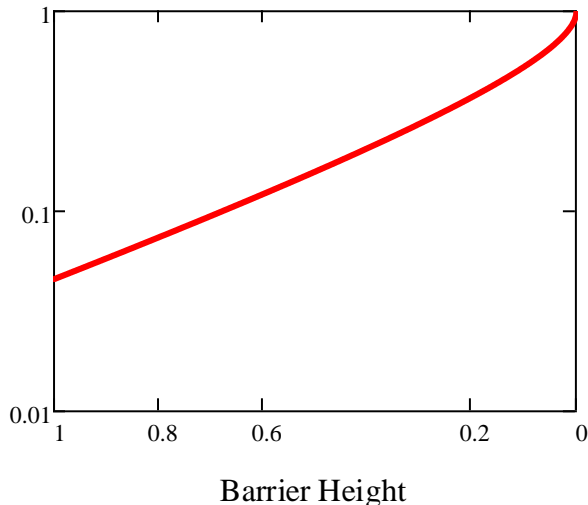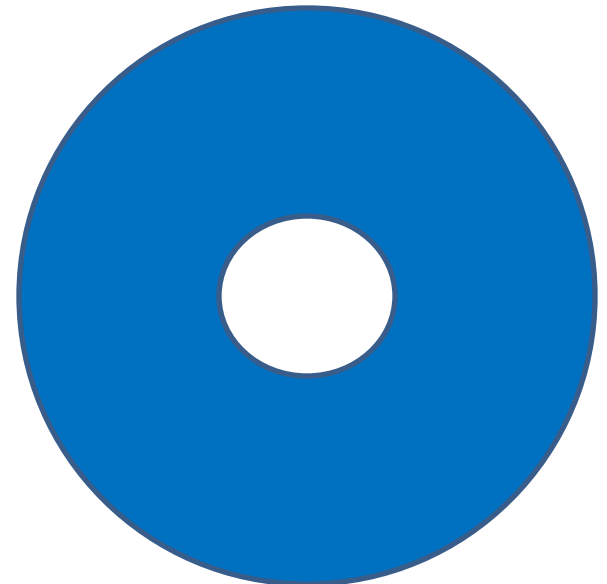
# Temperature Diagnostic: Useful Charge

- Initially, the plasma escapes from a central region on the order of several Debye lengths:

$$\lambda_D = \sqrt{\frac{\epsilon_0 k_B T}{n_0 e^2}}$$

- Eventually, the center erodes significantly.
- Once the center erodes, the subsequent charge contains little temperature information.
  - The rate at which the charge comes out is determined largely by the plasma self space charge.
- Because of the scaling of the Debye length with temperature, ever fewer particles contain temperature information as the temperature increases.
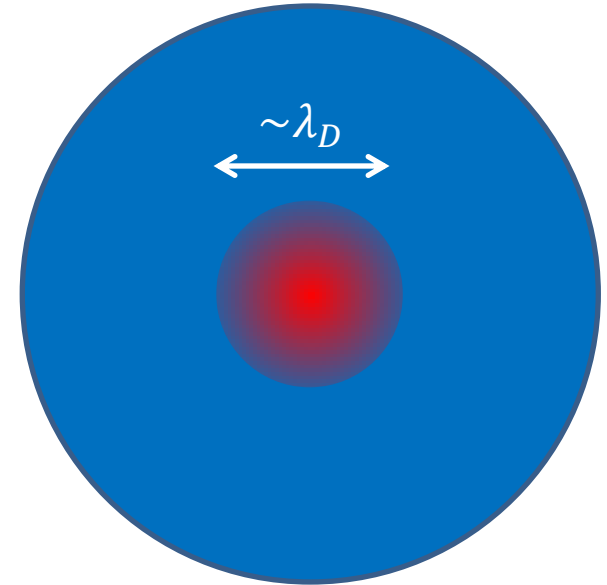
Plasma End View

D. L. Eggleston, C. F. Driscoll, B. R. Beck, A. W. Hyatt, and J. H. Malmberg, Parallel energy analyzer for pure electron plasma devices, Phys. Fluids B **4**, 3432 (1992).

B. R. Beck, Measurement of the magnetic and temperature dependence of the electron-electron anisotropic temperature relaxation rate, Ph.D Thesis, UCSD, 1990.

# Temperature Diagnostic: Antiproton Temperatures
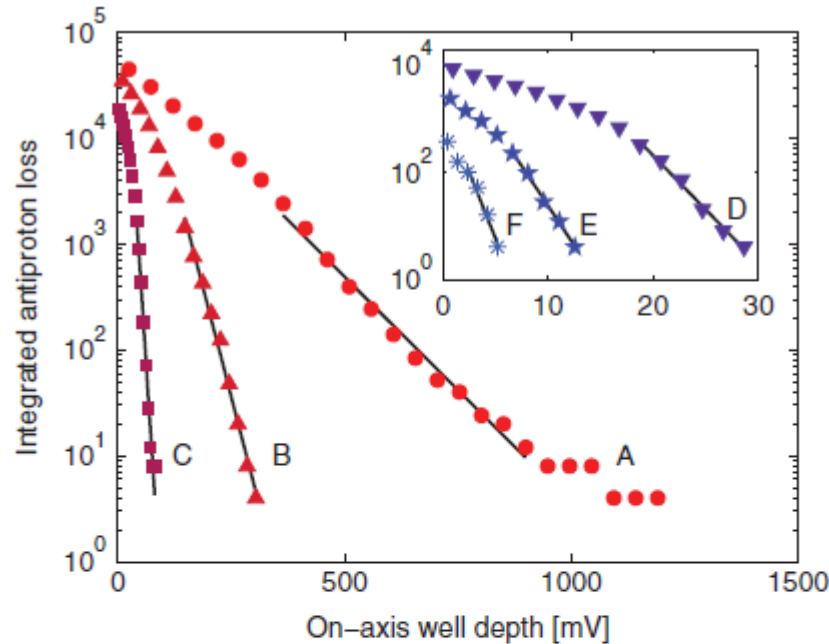
FIG. 2 (color). The number of antiprotons lost from the well as its depth is reduced is integrated over time and plotted against the well depth. The well depth is ramped from high to low; thus, time flows from right to left in the figure. The measured number is corrected for the 25% detection efficiency. The curves are labeled in decreasing order of the temperatures extracted from an exponential fit, shown as the solid lines. The temperatures (corrected as described in the text) are: A: 1040, B: 325, C: 57, D: 23, E: 19, and F: 9 K. As the antiprotons get colder, fewer can be used to determine their temperature, an effect described in Ref. [13].

Andresen et al (ALPHA Collaboration), Evaporative Cooling of Antiprotons to Cryogenic Temperatures, Phys. Rev. Lett., **105** 013003, 2010.

Temperature Diagnostic: Hot Lepton Temperatures
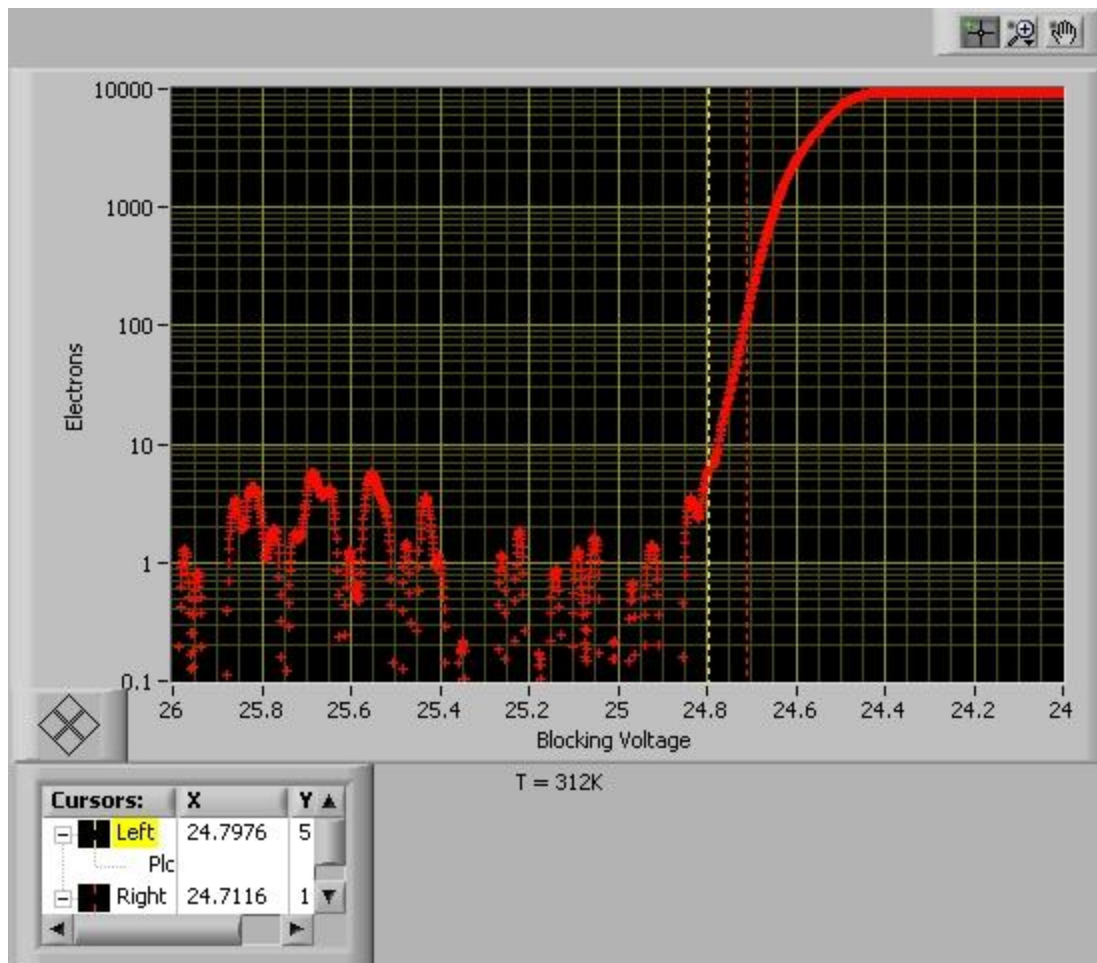
Temperature Diagnostic: Cold Lepton Temperatures
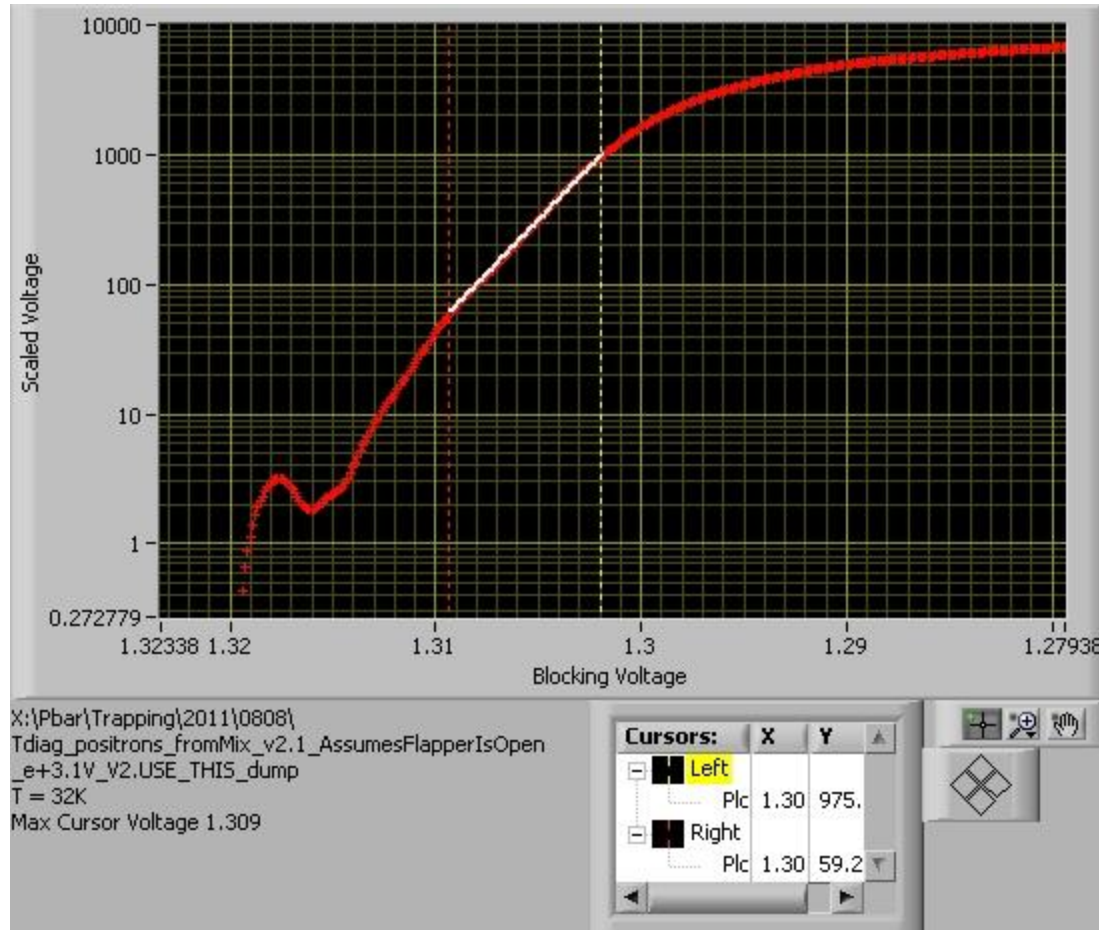
Temperature Diagnostic: Cold Temperatures and Noise
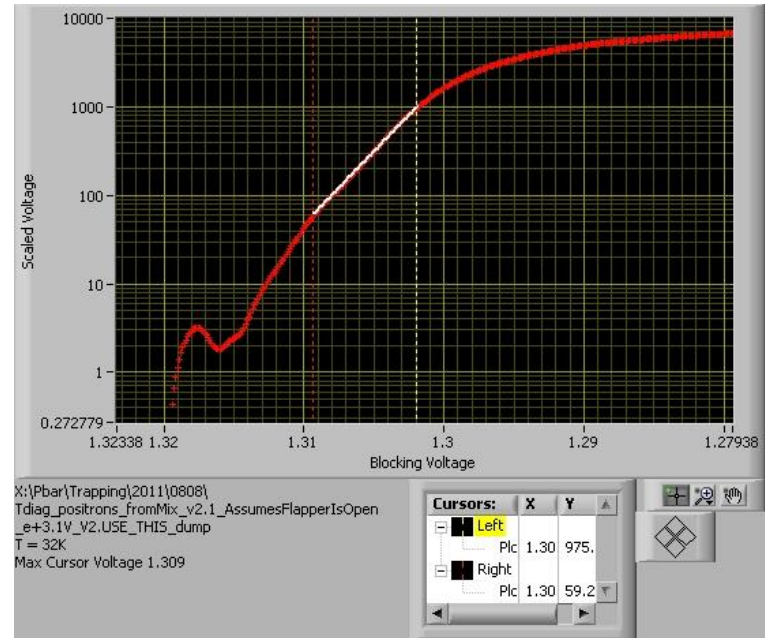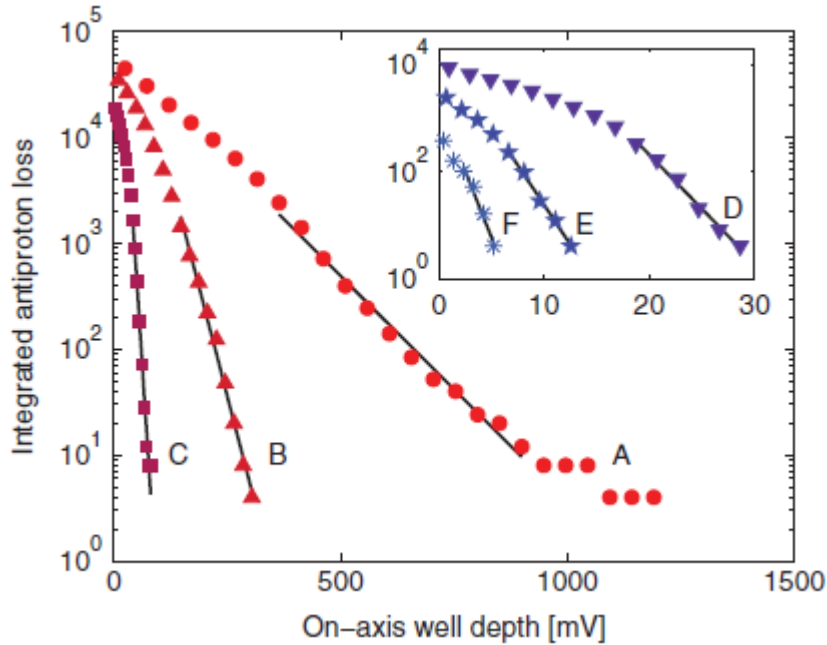
- The straight line region is short, and somewhat arbitrary at low temperatures.
  - Pickup and amplifier noise limits the bottom end.
  - Roll over from self potential effects limits the top end.
- To get into the tens of Kelvin region, one typically needs sensitivities on the order of hundreds to thousands of charges.

Temperature Diagnostic: Noise

- The base temperature that one can measure is limited by amplifier and pickup noise.
    - Acoustic noise from triboelectric effects is in the same band as the electrical pickup.
        - This is particularly a problem in cyrogenic experiments.
    - Consider:
        - Mounting amps very close to the pickup. This may mean that the amps are:
            - In vacuum.
            - At cryogenic temperatures.
    - Alpha uses a MCP preamp very successfully.

Temperature Diagnostic: Cold Temperatures and Noise
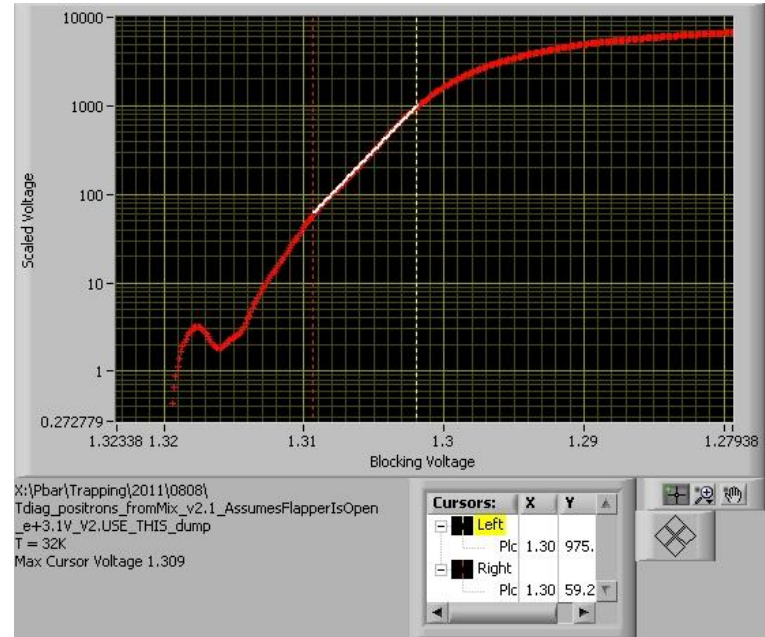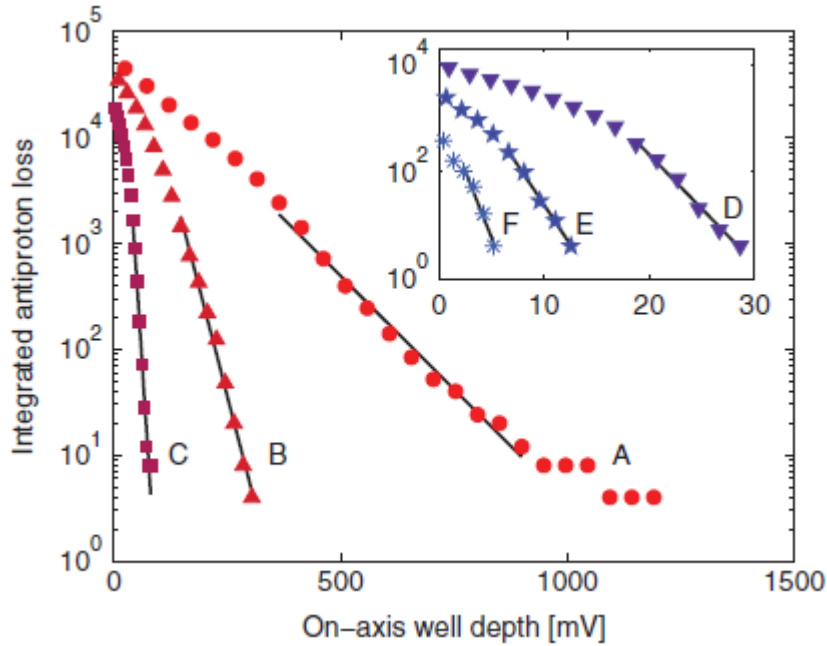
- Fitting a straight line seems arbitrary, but isn't.
- Fits are consistent to about 20%.
- Systematic effects are on the order of 20% to 100%.

Multi Species Temperature Diagnostic
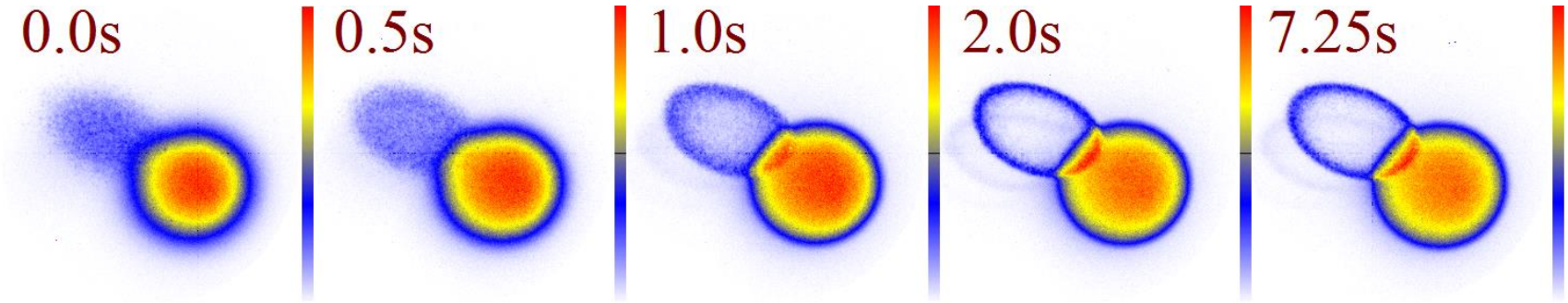
ALPHA, <u>Centrifugal Separation And Equilibration Dynamics In An Electron-Antiproton Plasma</u>, Phys. Rev. Lett. **106**, 145001 (2011)

As the plasma cools, it separates. Good, qualitative diagnostic.

Beam Temperature Diagnostic: Pepperpot

Beam emittance detector.

http://www.dreebit.com

http://www.dreebit.com

Pepperpot aperture

MCP

Phosphor screen

CCD camera

Macro zoom lens

Mirror

Ion beam

http://www.dreebit.com

Gauss fit rms = 13.9μm
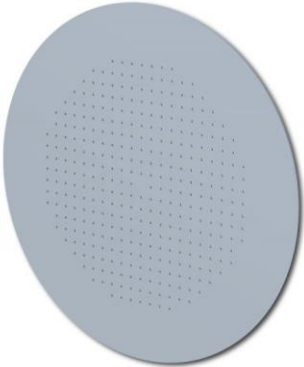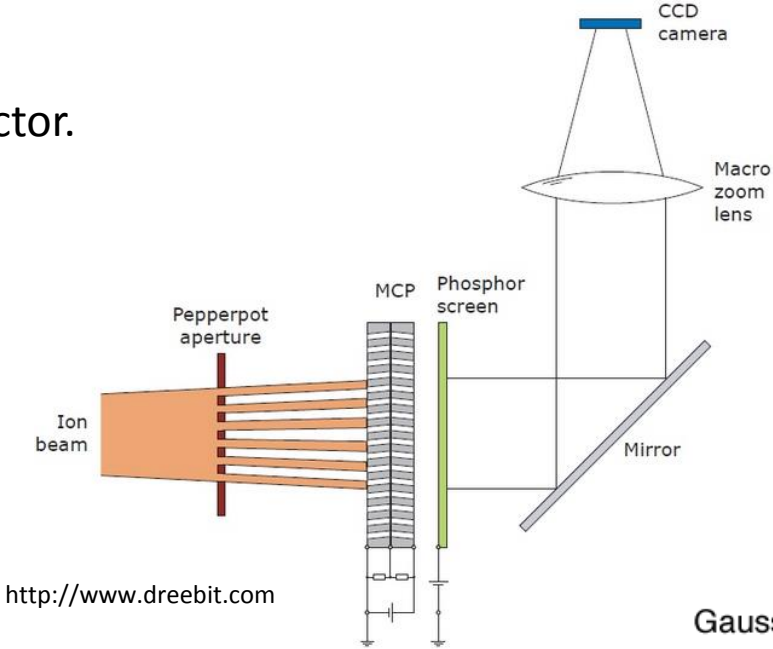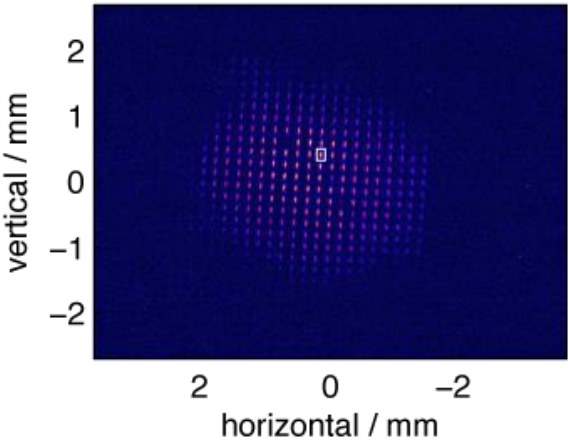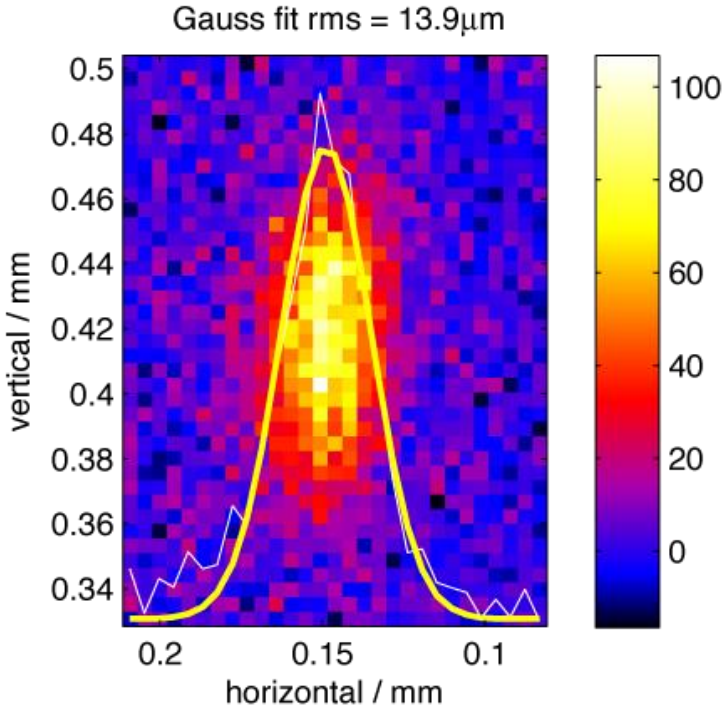
Nondestructive Diagnostics

- If you can't use lasers, how can you talk to a plasma?
- Use waves or modes.
    - Theory pioneered by Dan Dubin, and will be discussed by Francois.
    - Two modes particularly useful.
        - Sloshing mode: Used for calibration.
        - Breathing mode: Can be used to determine density, aspect ratio, temperature.
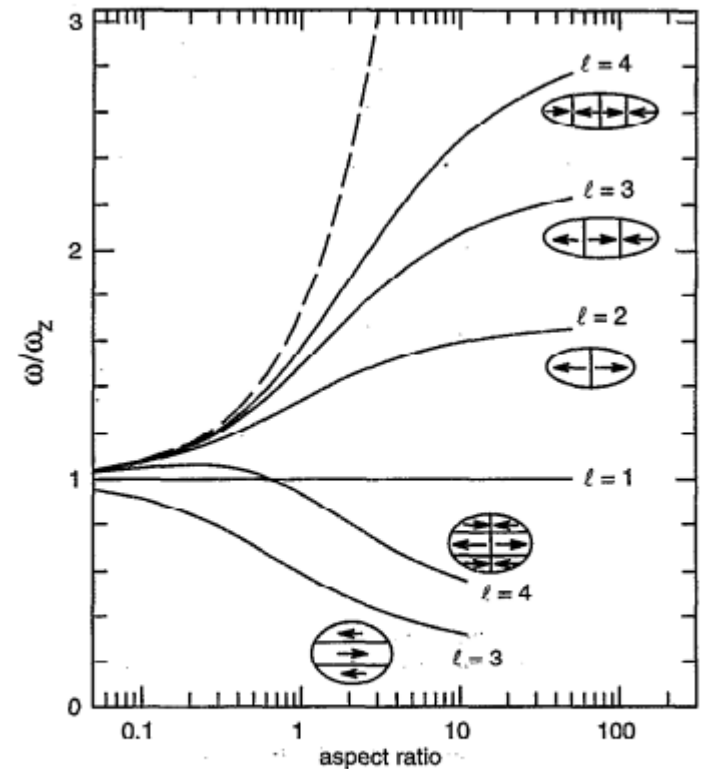
FIG. 2. Cold fluid theory for axial modes of highly magnetized spheroidal plasmas: frequency as a function of aspect ratio for several low-order modes, scaled by ω_z. The dashed line is the plasma frequency.

M.D. Tinkle, R.G. Greaves, C. Surko, Lower order longitudinal modes of single-component plasmas. Phys. Plasmas, **2**, 2880, (1995).

Modes Diagnostics

- Put a plasma into a harmonic well.
  - Actually, doesn't need to be too harmonic
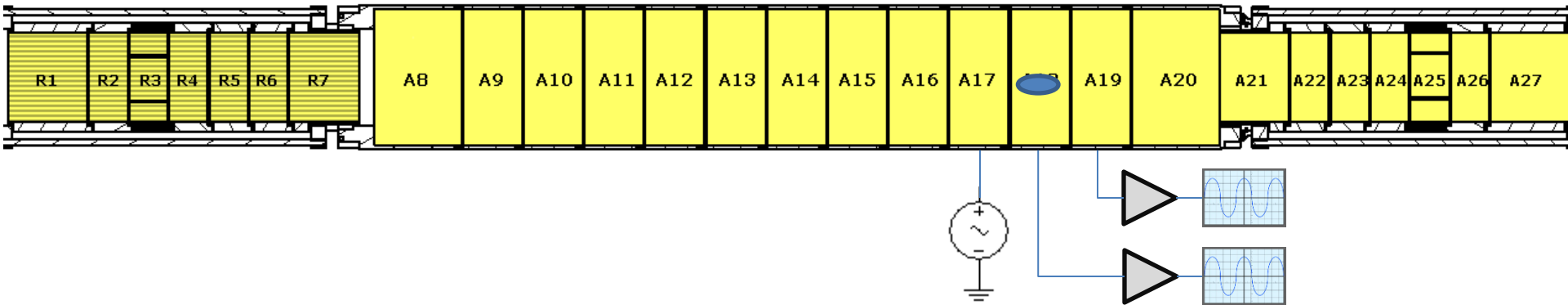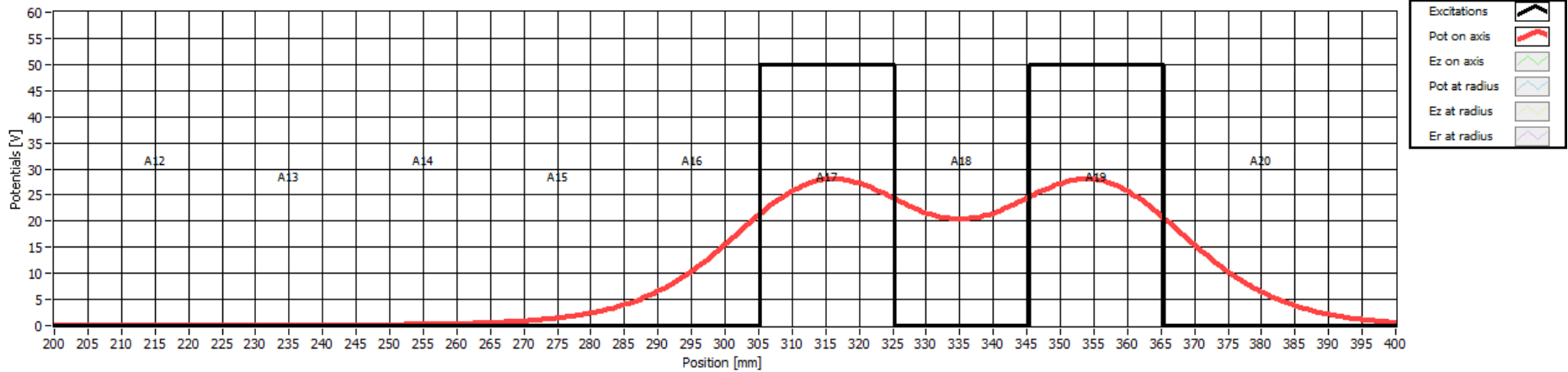
Which pickup is used for which mode?

Modes Diagnostics

- Measure the frequencies of both modes.
- Measure the total charge.
- From these measurements, use some somewhat nasty equations involving Legendre functions of the first and second kind to determine the aspect ratio, length and density of the plasma.
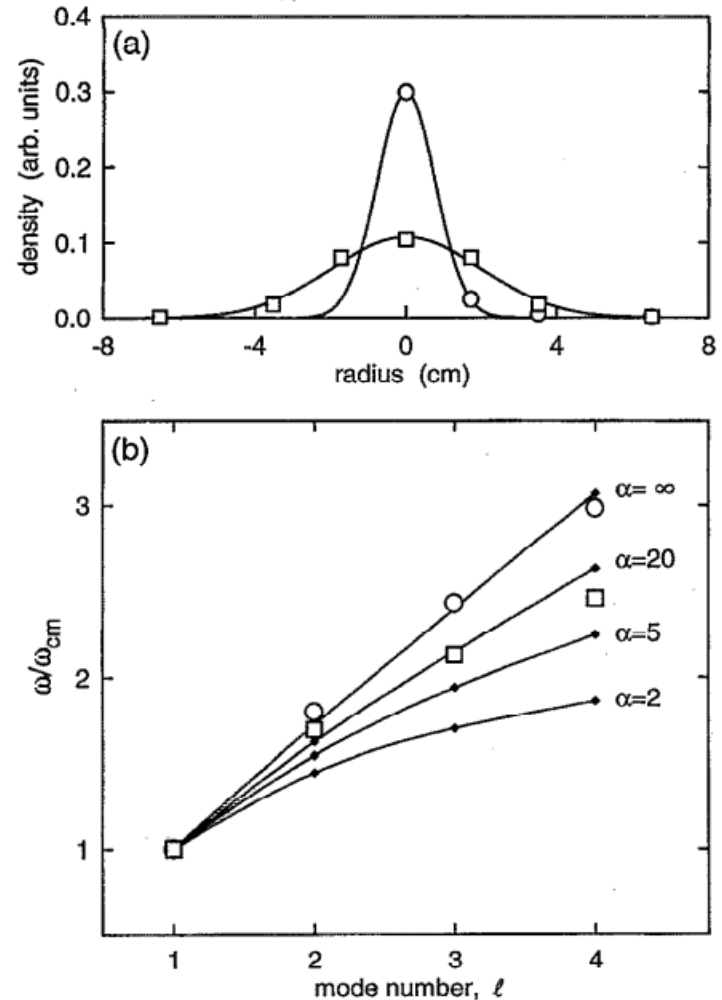

FIG. 10. (a) The z-integrated radial profiles for two plasmas in the cylindrical trap with similar numbers of particles and different aspect ratios: (O) $\alpha \sim 20$; (□) $\alpha \sim 5$. (b) Comparison of the frequencies of four modes in the plasmas shown in (a) with spheroidal mode theory shown by small points connected by smooth curves.

M.D. Tinkle, R.G. Greaves, C. Surko, Lower order longitudinal modes of single-component plasmas. Phys. Plasmas, **2**, 2880, (1995).

Modes Diagnostics

- Closer look:
  - The theory predicts the mode frequency well, particularly for the second mode. (The first mode is used for calibration, and is defined to be exact.)
  - The inverse prediction, which is what we want, is not particularly good.
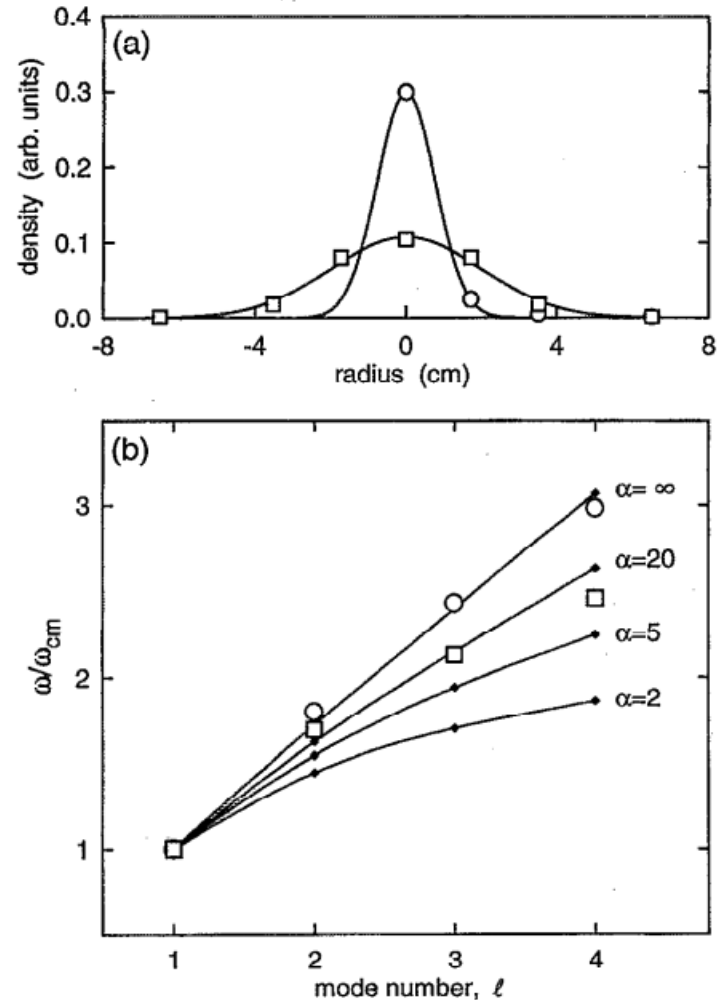

FIG. 10. (a) The z-integrated radial profiles for two plasmas in the cylindrical trap with similar numbers of particles and different aspect ratios: (O) $\alpha{\sim}20$; (□) $\alpha{\sim}5$. (b) Comparison of the frequencies of four modes in the plasmas shown in (a) with spheroidal mode theory shown by small points connected by smooth curves.

M.D. Tinkle, R.G. Greaves, C. Surko, <u>Lower order longitudinal modes of single-component</u> plasmas. Phys. Plasmas, **2**, 2880, (1995).

Modes Diagnostics

- Why is the inverse prediction off?
  - The equations are numerically unstable, particularly for high aspect ratio plasmas (high α).
  - The equations do not take into account the trap wall, which has significant effect.
    - Numerical solutions have been attempted, but the inclusion of these effects is variously reported as "essentially impossible"[1] and straightforward.[2]
    - In my personal experience, the inversion problem does not satisfy elementary self-consistency checks for high α plasmas. Others disagree.
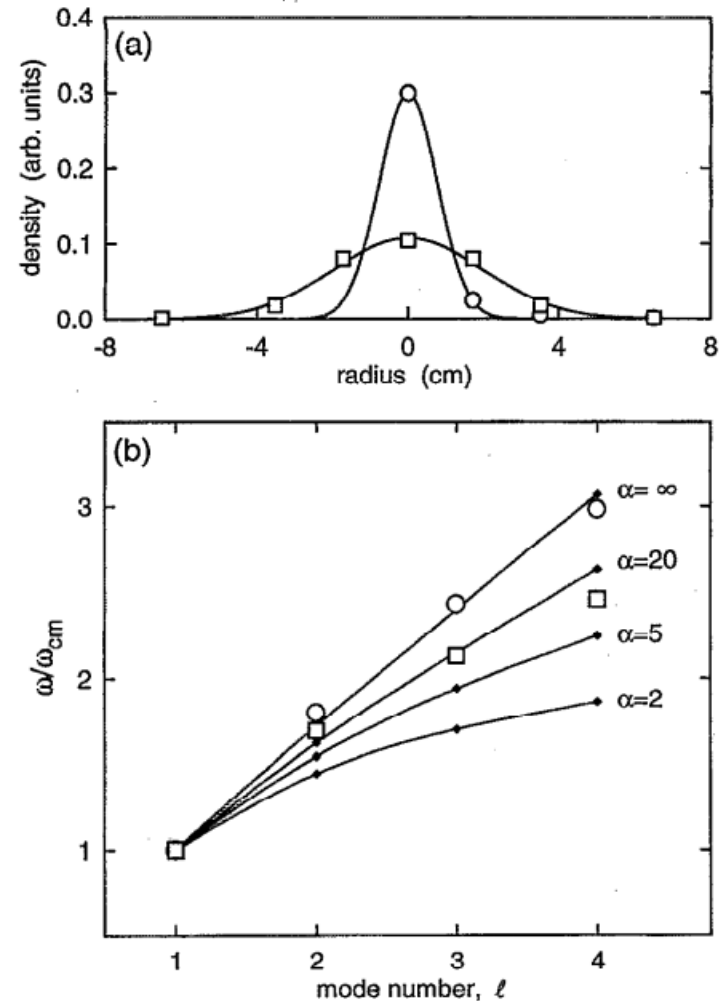
[1]Francis Robicheaux, personal communication.
[2]Speck, Density and geometry of single component plasmas, Phys. Lett. B, **650**, 119 (2007).

FIG. 10. (a) The z-integrated radial profiles for two plasmas in the cylindrical trap with similar numbers of particles and different aspect ratios: (O) $\alpha \sim 20$; (□) $\alpha \sim 5$. (b) Comparison of the frequencies of four modes in the plasmas shown in (a) with spheroidal mode theory shown by small points connected by smooth curves.

M.D. Tinkle, R.G. Greaves, C. Surko, Lower order longitudinal modes of single-component plasmas. Phys. Plasmas, **2**, 2880, (1995).

Modes Diagnostics

- Why is the inverse prediction off?
  - The basic theory assumes the plasmas are cold.
  - The theory has been extended for warm plasmas.
 - This makes for a useful, **relative**, temperature diagnostic.
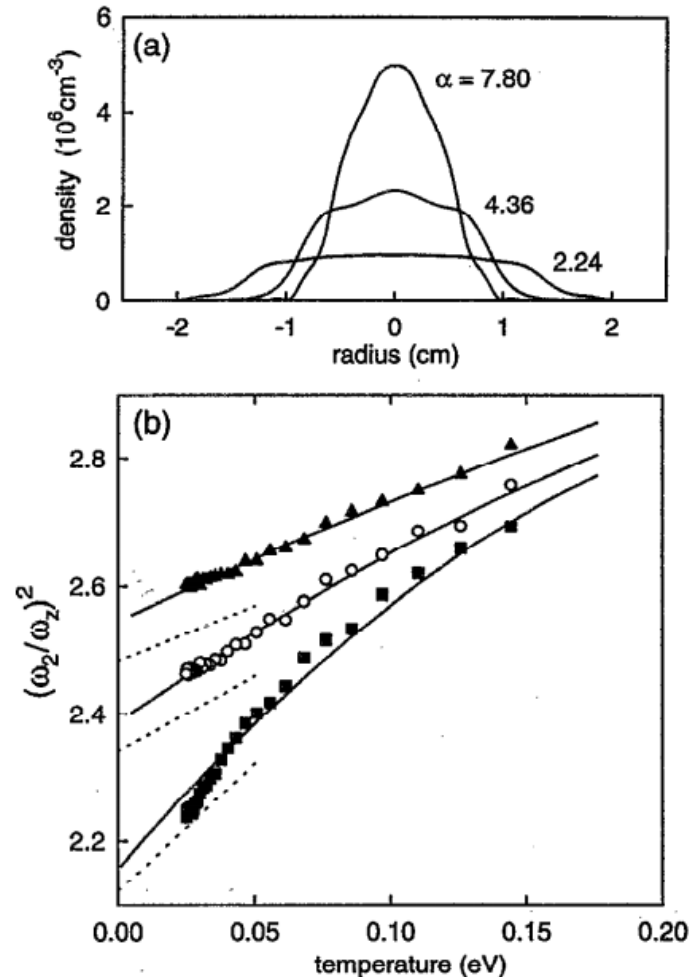
FIG. 14. (a) Radial density profiles in the plasma midplane for three electron plasmas with similar numbers of particles but different aspect ratios. (b) Temperature dependence of the quadrupole mode frequency for the plasmas shown in (a): (□) $\alpha=2.24$, $L=6.20$ cm; (○) $\alpha=4.38$, $L=7.52$ cm; (△) $\alpha=7.80$, $L=8.32$ cm. The solid lines are numerical simulations and the dotted lines are from the fluid theory using Eq. (19).

M.D. Tinkle, R.G. Greaves, C. Surko, Lower order longitudinal modes of single-component plasmas. Phys. Plasmas, **2**, 2880, (1995).

Modes Temperature Diagnostic

- The modes are a useful, **relative**, temperature diagnostic.
  - Base Δf_2 is unknown.
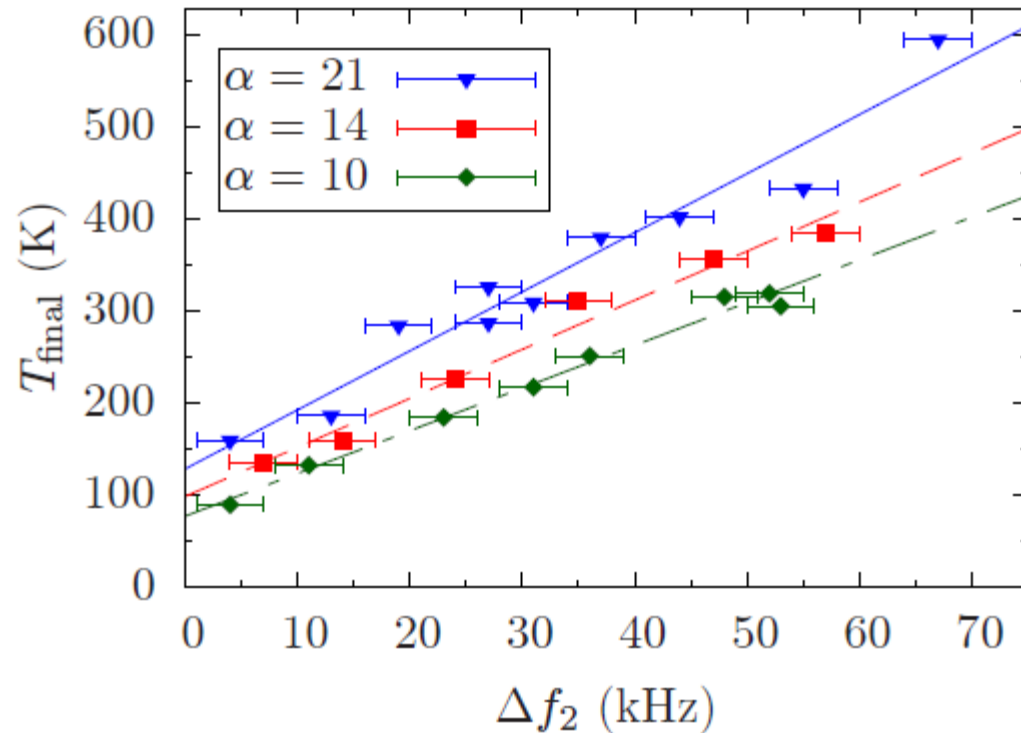
ALPHA, <u>In situ electromagnetic field diagnostics with an electron plasma in a Penning–Malmberg</u> trap, New J. Phys., **16**, 013037 (2014).

Thermal Modes Diagnostics

- Using nontrivial apparatus, the thermal spectrum of the mode in the plasma can be measured.

N. Shiga, F. Anderegg, D.H.E. Dubin, C.F. Driscoll and R.W. Gould , Thermally excited fluctuations as a pure electron plasma temperature diagnostic, Phys. Plasmas **13**, 022109:, (2006).
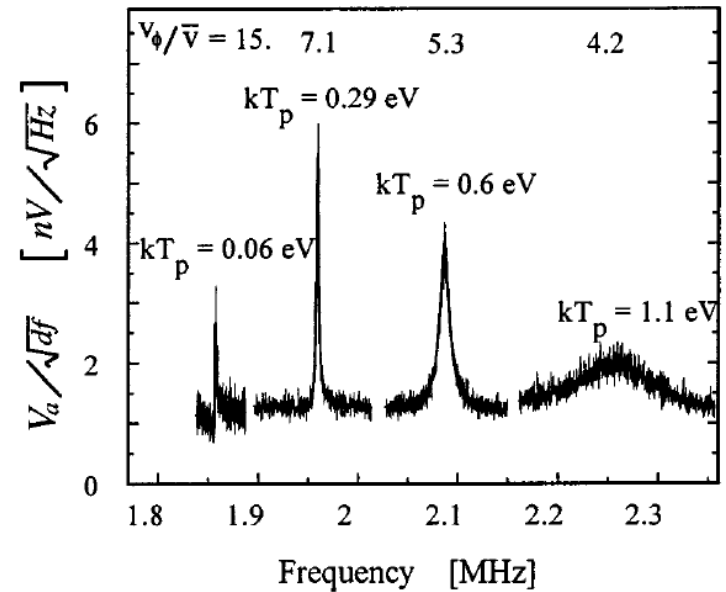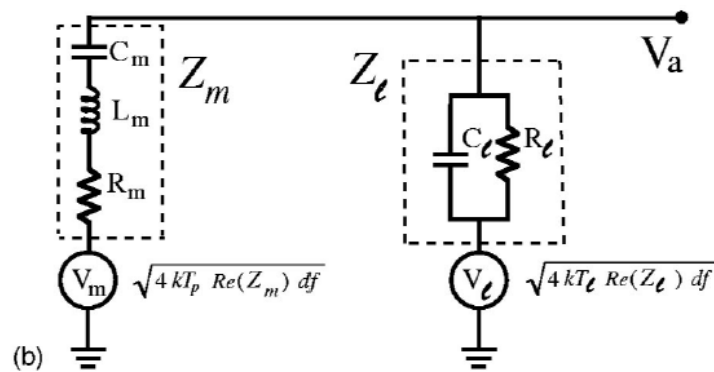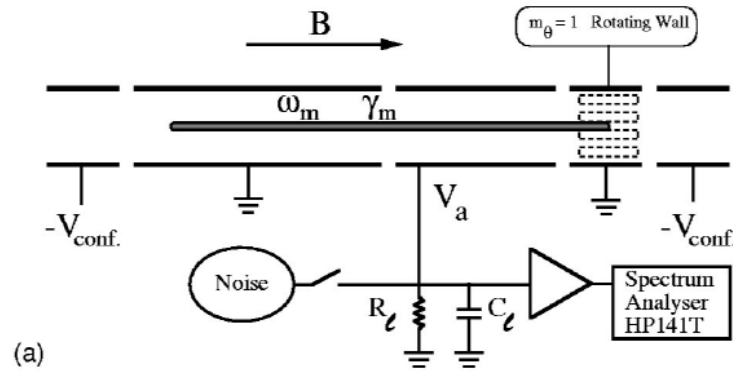
Thermal Modes Diagnostics

- Using nontrivial apparatus, the thermal spectrum of the mode in the plasma can be measured.
- From the power in the spectra, the temperature can be inferred.
- This is the perfect nondestructive temperature diagnostic…
  - Except:
    - Calibration is difficult.
    - Probably requires a very quiet environment.
    - May require amplifiers whose noise temperature is lower than the temperature of the plasmas under measurement.
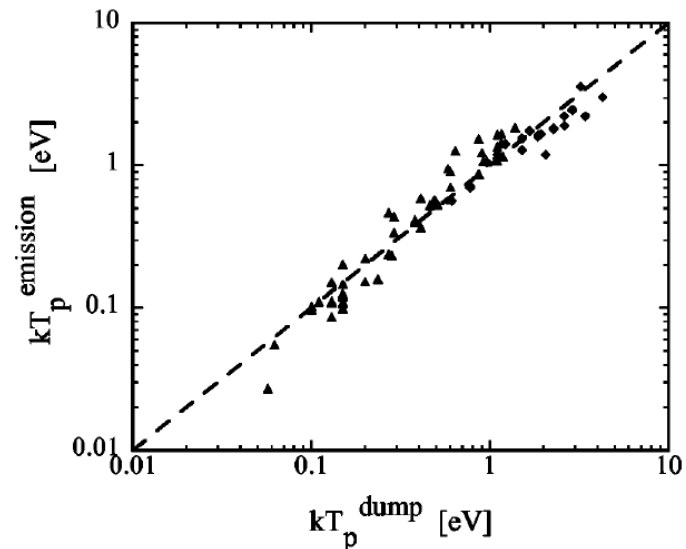
N. Shiga, F. Anderegg, D.H.E. Dubin, C.F. Driscoll and R.W. Gould , Thermally excited fluctuations as a pure electron plasma temperature diagnostic, Phys. Plasmas **13**, 022109:, (2006).

Thermal Modes Diagnostics

Using nontrivial apparatus, the thermal spectrum of the mode in the plasma can be measured

N. Shiga, F. Anderegg, D.H.E. Dubin, C.F. Driscoll and R.W. Gould , Thermally excited fluctuations as a pure electron plasma temperature diagnostic, Phys. Plasmas **13**, 022109:, (2006).
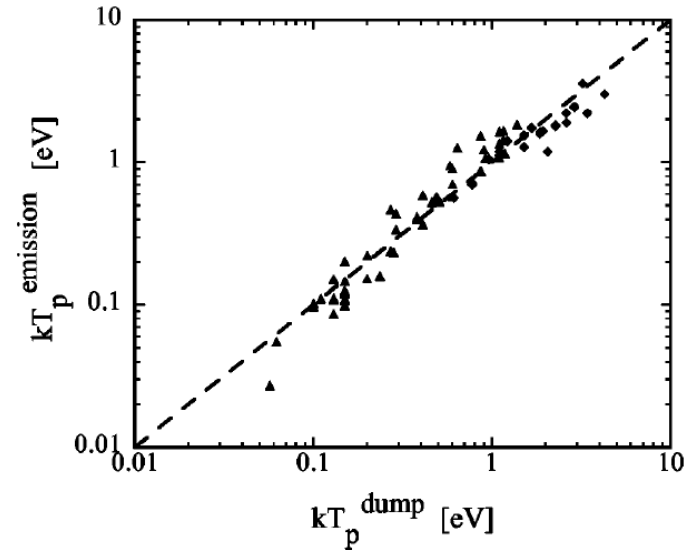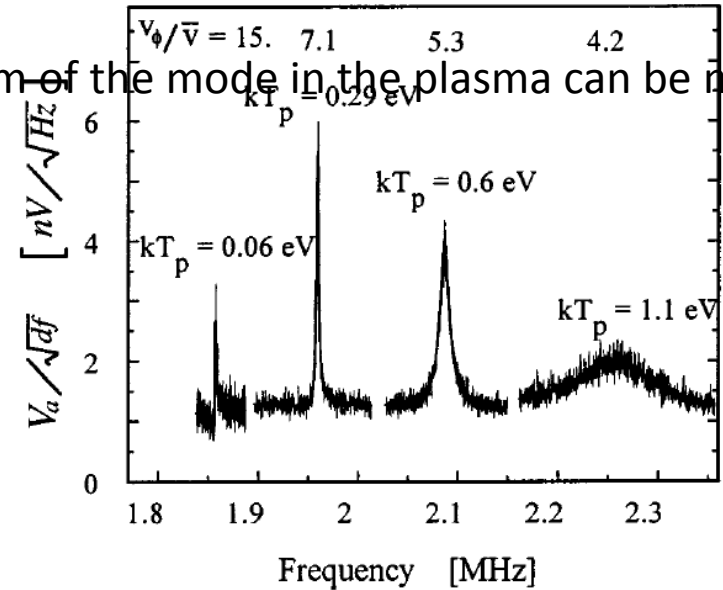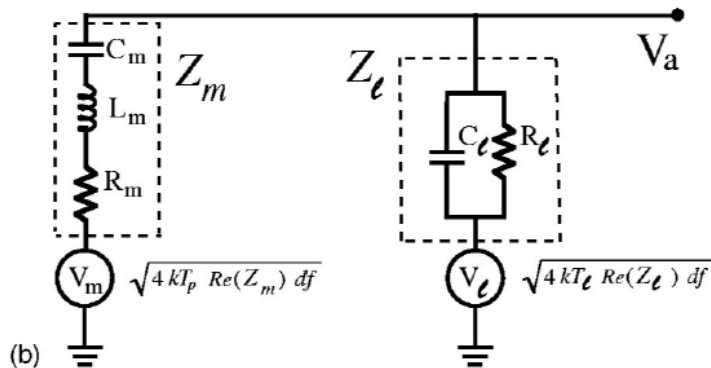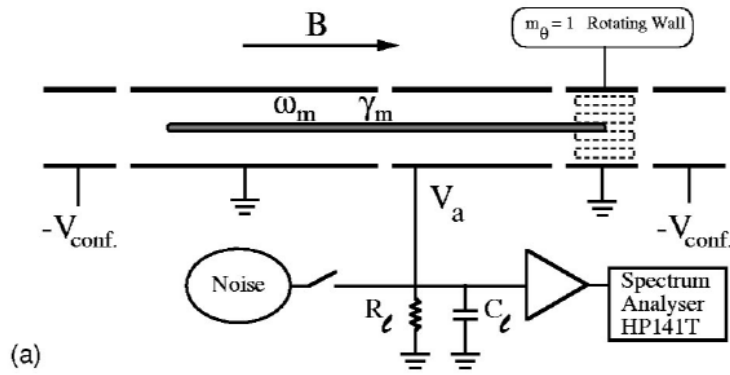
At 20:40 Saturday, right here.

Movies

Cartoons

No Math

Two Dimensional Fluid Motion
in Non-Neutral Plasmas